Identification and Optimization of New Dual Inhibitors of B-Raf and Epidermal Growth Factor Receptor Kinases for Overcoming Resistance against Vemurafenib

ARTICLE *in* JOURNAL OF MEDICINAL CHEMISTRY · MARCH 2014

Impact Factor: 5.45 · DOI: 10.1021/jm500007h · Source: PubMed

Journal of Medicinal Chemistry

Article

pubs.acs.org/jmc

Identification and Optimization of New Dual Inhibitors of B-Raf and Epidermal Growth Factor Receptor Kinases for Overcoming Resistance against Vemurafenib

Huimin Cheng,[†,∥] Yu Chang,[‡,∥] Lianwen Zhang,[†,∥] Jinfeng Luo,[†] Zhengchao Tu,[†] Xiaoyun Lu,[†] Qingwen Zhang,[‡] Jibu Lu,[§] Xiaomei Ren,[†] and Ke Ding*[,†]

[†]Institute of Chemical Biology, Guangzhou Institutes of Biomedicine and Health, Chinese Academy of Sciences, #190 Kaiyuan Avenue, Guangzhou 510530, China

[‡]University of Macau, Avenue Padre Tomás Pereira Taipa, Macau, China

[§]Shenyang Pharmaceutical University, #103 Wenhua Road, Shenyang 110016, China

Supporting Information

ABSTRACT: Epidermal growth factor receptor (EGFR) amplification has been demonstrated to be critical for the inherent and/or acquired resistance against current B-Raf^{V600E} inhibitor therapy for melanoma and colorectal cancer patients. We describe the discovery and structure−activity relationship study of a series of 1*H*-pyrazolo[3,4-*b*]pyridine-5-carboxamide analogues as novel dual inhibitors of EGFR and B-Raf^{V600E} mutant. One of the most promising compounds, **6a**, potently inhibited both of the kinases with IC_{50} values of 8.0 and 51 nM, respectively. The compound also strongly suppressed the proliferation of a panel of intrinsic and acquired resistant melanoma and/or colorectal cancer cells harboring overexpressed EGFR with submicromolar IC_{50} values. Further mechanism investigation revealed that **6a** could sustainably inhibit the activation of the MAPK path way in the resistant SK-MEL-28 PR30 melanoma cancer cells and WiDr colorectal cancer cells with EGFR amplification. Our results support the hypothesis that the EGFR/B-Raf^{V600E} dual inhibition might be a tractable strategy to overcome the intrinsic and acquired resistance of melanoma and/or colorectal cancers against the current B-Raf^{V600E} inhibitor therapy.

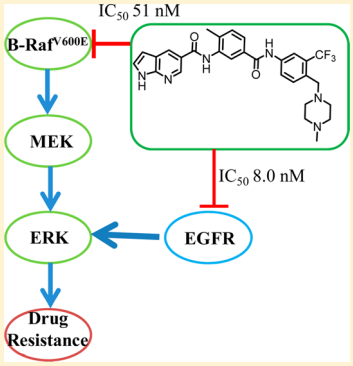

INTRODUCTION

The Raf proteins belong to a serine/threonine kinase family and are critical components in the mitogen activated protein kinase (MAPK) signal transduction pathway.[1,2] Three isoforms of Raf kinase, i.e., A-Raf, B-Raf, and C-Raf, have been identified.[3] Aberrant activation and/or constitutively activating mutation of Raf kinase have been linked with multiple types of cancers.[4] In particular, B-Raf mutations have been identified in various cancers including malignant melanoma (50−60%), papillary thyroid (30−50%), colorectal (10−15%), and lung (~3%) cancers, hairy cell leukemia (~100%), and others.[5−7] The Val ^{600} → Glu ^{600} (V600E) transition is the most common mutation and accounts for over 90% in all of the B-Raf oncogenic mutants reported to date. The identification of B-Raf mutation in multiple human cancers promoted the extensive efforts to develop B-Raf inhibitors as new potential antitumor agents.[8,9] Recently, two selective B-Raf inhibitors, vemurafenib (**1**, PLX4032)[10] and dabrafinib (**2**),[11] were approved by the US Food and Drug Administration (FDA) for the management of late-stage or unresectable melanoma harboring B-Raf^{V600E} mutation (Figure 1).[12,13] The drugs have achieved remarkable clinical benefit for melanoma patients with B-Raf^{V600E} mutation.[14] For instance, drug **1** treatment produces a 60−80% overall response rate and a median progression-free survival of approximately 7 months in the B-Raf^{V600E} mutated melanoma patients.[15,16] The similar clinical efficacy has also been reported for drug **2**.[17,18]

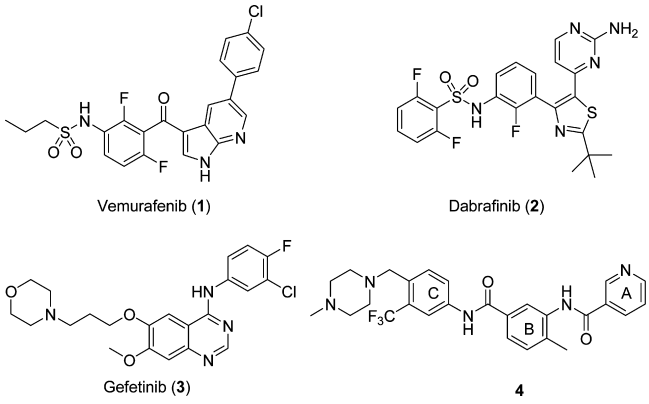

Figure 1. Chemical structures of FDA approved B-Raf^{V600E} inhibitors vemurafenib (**1**) and dabrafinib (**2**), EGFR inhibitor gefitinib (**3**), and the new B-Raf/EGFR dual inhibitor **4**.

Although the antitumor effects of drugs **1** and **2** in melanoma are highly promising, intrinsic and acquired resistance limits the

Received: January 3, 2014
Published: March 3, 2014

Scheme 1. Syntheses of Compounds 4, 5, and 6[a]

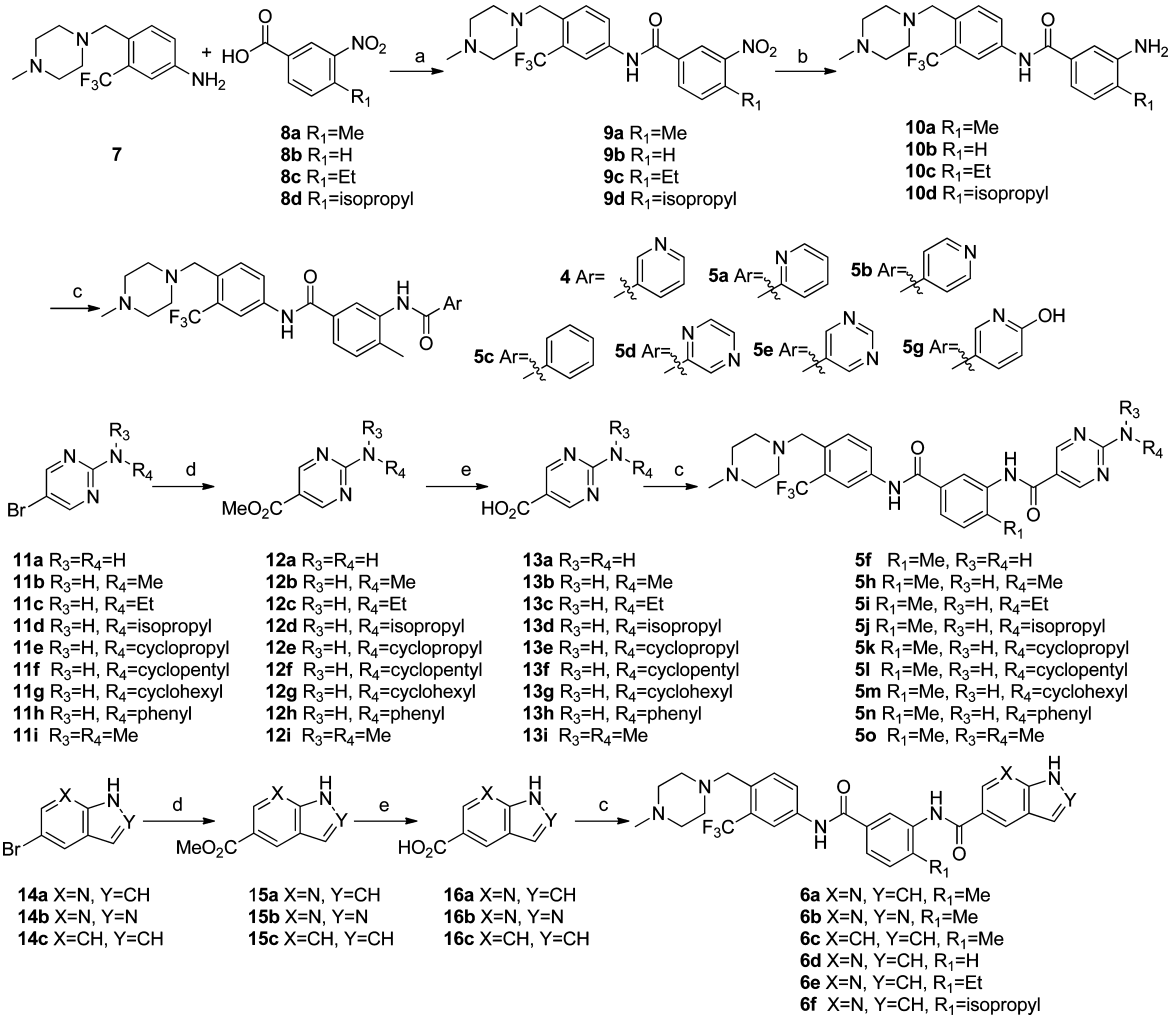

[a]Reagents and conditions: (a) PyBOP, Et_3N, THF, rt, 12 h, 46−85%; (b) H_2, 10% Pd/C, CH_3OH, rt, 8 h, 68−92%; (c) HATU, DIEA, DMF, rt, 12 h, 47−62%; (d) $Pd(OAc)_2$, 4,5-bis(diphenylphosphino)-9,9-dimethylxanthene, Et_3N, CH_3OH, CO, 100 °C, 12 h, 52−83%; (e) LiOH, MeOH:THF:H_2O (1:1:2), rt, 3.0 h, 44−89%.

therapeutic benefit of current drugs.[19−31] For instance, a majority of colorectal cancer patients display inherent resistance against drug **1**, although they were detected to harbor B-Raf^{V600E} mutation, and the overall response rate is less than 5% in a clinical investigation.[32] The exact mechanism for the significant difference in the efficacy of drug **1** between B-Raf^{V600E} mutated colorectal cancer and melanomas remains elusive. The most recent results from two independent groups strongly suggested that the epidermal growth factor receptor (EGFR) activation might be a critical cause of the inherent resistance against B-Raf^{V600E} inhibition in colorectal cancer.[25,26] A combinational therapy of drug **1** with an EGFR inhibitor has been conducted to effectively overcome the resistance both *in vitro* and *in vivo*. More encouragingly, a clinically successful case for the off-label combination of cetuximab (an EGFR monoclonal antibody) with sorafenib (a Raf inhibitor) to treat the metastatic colorectal cancer patient with B-Raf^{V600E} mutation was recently reported.[33] It was also demonstrated that upregulation of v-erb-b2 avian erythroblastic leukimia viral congene homologue 3 (ERBB3), another member of EGFR kinase family, contributes greatly to the adaptive resistance of melanoma against drug **1**. Combination of drug **1** with an ERBB2/EGFR inhibitor lapatinib successfully reduced tumor burden and extended latency of tumor growth in both cultured cancer cells and mouse xenograft models through inactivation of the ERBB3 signal.[34] Combinational therapy of FDA approved drugs with different mechanisms of action (MOA) is a powerful strategy for the treatment of various cancers.[35,36] However, a synergistic hepatotoxicity was observed in melanoma patients after combinational treatment of drug **1** with another FDA approved antimelanoma antibody ipilimumab, suggesting the requirement of careful protocol design for combinational therapies to avoid the potential drug−drug interaction.[37] Thus, dual inhibition of B-Raf and EGFR by using a single compound may provide a novel promising and manageable strategy for the treatment of colorectal cancer patients with B-Raf^{V600E} mutation.

Several molecules have been reported to show nonselective dual inhibition against both B-Raf and EGFR kinases.[38,39] However, to the best of our knowledge, there is rarely a successful report on the treatment of intrinsic resistant colorectal cancers by using a B-Raf/EGFR dual inhibitor. Herein, we would like to describe the discovery of a class of 1*H*-pyrazolo[3,4-*b*]pyridine-5-carboxamides as novel dual inhib-

dx.doi.org/10.1021/jm500007h | *J. Med. Chem.* 2014, 57, 2692−2703

Table 1. *In Vitro* Kinase Inhibitory Activities of the New Inhibitors against B-Raf ^{V600E} and EGFR and Their Antiproliferation Effects

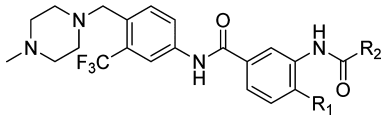

Compd	R^1	R^2	Kinase inhibition (IC_{50}, μM) B-Raf ^{V600E} [a]	Kinase inhibition (IC_{50}, μM) EGFR [b]	Cell growth inhibition (IC_{50}, μM) [c] SK-MEL-28	Cell growth inhibition (IC_{50}, μM) [c] SK-MEL-28-PR30
1			0.026	> 10	0.48±0.03	> 20
3			2.00	0.001	> 20	> 20
4	Me		0.551	0.550	13.98±1.13	>20
5a	Me		0.573	0.575	>20	10.73±1.65
5b	Me		0.11	> 10	>20	>20
5c	Me		0.24	> 10	6.91±1.30	5.03±0.87
5d	Me		0.28	3.90	>20	>20
5e	Me		0.67	1.92	>20	>20
5f	Me		0.41	0.043	1.84±0.69	1.89±0.53
5g	Me		> 10	1.33	>20	>20
5h	Me		0.29	0.12	>20	2.75±0.74
5i	Me		0.51	0.13	1.09±0.23	2.40±0.29
5j	Me		0.34	0.043	1.73±0.20	0.86±0.08
5k	Me		0.39	0.044	2.96±0.37	1.44±0.11
5l	Me		0.23	0.033	2.04±0.14	1.24±0.42
5m	Me		0.037	0.047	2.38±0.30	2.73±0.29
5n	Me		0.21	0.006	1.70±0.19	0.90±0.09
5o	Me		0.30	5.54	6.96±0.09	2.49±0.22
6a	Me		0.051	0.008	**0.13±0.06**	**0.45±0.02**
6b	Me		0.048	0.030	**0.54±0.16**	**0.78±0.11**
6c	Me		0.22	> 10	4.43±0.37	3.04±0.16
6d	H		0.048	0.68	1.07±0.12	1.73±0.13
6e	Et		0.36	0.099	0.91±0.42	0.49±0.01
6f	$(CH_3)_2$ CH		0.29	0.16	2.27±0.47	1.90±0.47

[a] B-Raf ^{V600E} kinase activity assays were performed using the FRET-based Z′-Lyte assays according to the manufacturer's instructions.[44] The compounds were incubated with the kinase reaction mixture for 1−1.5 h before measurement. Reported data are the means from 2 independent experiments. [b] EGFR kinase activity assays were performed using the FRET-based Z′-Lyte assays according to the manufacturer's instructions.[44] The compounds were incubated with the kinase reaction mixture for 1−1.5 h before measurement. Reported data are the means from 2 independent experiments. [c] The antiproliferative activities of the compounds were evaluated using the MTS assay. Data are reported as the means ± SDs (standard deviations) from at least three independent experiments.

itors of B-Raf^{V600E} and EGFR kinases. The compounds potently inhibited the kinase activities of both B-Raf^{V600E} and EGFR with low nanomolar IC_{50} values. Furthermore, the compounds also displayed potent inhibition on the proliferation of a panel of vemurafenib-resistant cancer cells with high levels of EGFR, representing new leads for further development of B-Raf/EGFR dual inhibitors to overcome the resistance against FDA approved drug **1**.

CHEMISTRY

The synthesis of compounds **4**, **5a−o**, and **6a−f** is illustrated in Scheme 1. Briefly, commercially available compound **7** was coupled with different carboxylic acids **8** under the catalysis of benzotriazol-1-yl-oxytripyrrolidinophosphonium hexafluorophosphate (PyBOP) to produce the benzamides **9**. Compounds **9** were hydrogenated to provide the anilines **10**. Compounds **10** could react with different aromatic acids **13** or **16** to afford the final products **4**, **5a−o**, and **6a−f** by using another coupling reagent 1-[bis(dimethylamino)methylene]-1*H*-1,2,3-triazolo-[4,5-b]pyridinium 3-oxid hexafluorophosphate (HATU). It was noteworthy that the amino group in **13a** should be protected with the butoxycarbonyl group before it could effectively couple with the aniline **10** to afford inhibitor **5f**. The commercially unavailable intermediates **13** and **16** could be readily prepared by using compounds **11** or **14**, respectively, by utilizing the Pd-catalyzed carbonyl insertion coupling reaction,[40] followed by standard hydrolysis.

dx.doi.org/10.1021/jm500007h | J. Med. Chem. 2014, 57, 2692−2703

Chart 1. Strategies for the Structural Optimization of Initial "Hit" Compound 4

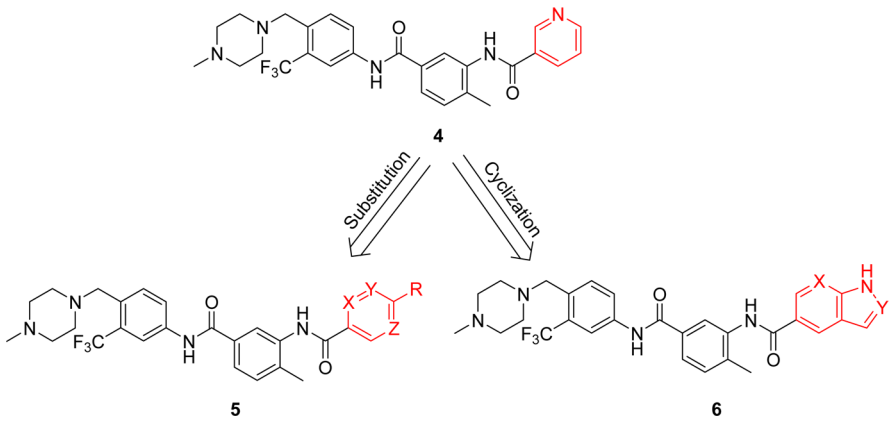

RESULTS AND DISCUSSION

In order to identify novel B-Raf/EGFR dual inhibitors for overcoming the intrinsic resistance of colorectal cancers against the current B-Raf inhibitor therapy, we conducted a random screening on our self-constructed-kinase-inhibitor focused library. Compound **4** was discovered to display good inhibitory activities against both B-Raf^{V600E} and EGFR, with IC_{50} values of 551 nM and 550 nM, respectively (Table 1). Similar to the reported data, drug **1** potently inhibits the kinase activity of B-Raf ^{V600E} mutant with an IC $_{50}$ value of 26 nM,[41] but it is almost totally inactive against EGFR. However, gefitinib (**3**), an FDA approved EGFR inhibitor, strongly inhibits EGFR with a 1.0 nM IC_{50} value,[42,43] but its potency on B-Raf is minor.

Extensive structural optimization of the lead compound (**4**) was conducted to improve its dual inhibition against EGFR and B-Raf^{V600E} (Chart 1) and the results are summarized in Table 1. We first investigated the potential impact of the nitrogen atom in aromatic ring A of compound **4** on its dual inhibition against EGFR and B-Raf ^{V600E} kinases by altering the position of the N-atom. It was found that the position of the N-atom displayed diverse effects on the inhibitory activity on EGFR and B-Raf ^{V600E}. Although the 2-pyridinylcarboxyl-derivative (**5a**) displayed similar potencies on both EGFR and B-Raf ^{V600E} to that of compound **4**, the 4-pyridinylcarboxyl-compound **5b** totally lost its suppressive effect on EGFR, while its inhibitory potency on B-Raf^{V600E} was improved about 5-fold. Interestingly, the benzamide compound **5c** also selectively suppressed the kinase function of B-Raf^{V600E} with an IC_{50} value of 240 nM, while the inhibitory effect on EGFR was totally abolished. Pyrazine-2-carboxamide (**5d**) and pyrimidine-5-carboxamide (**5e**) analogues were also designed and synthesized. Both of the compounds showed moderate inhibitory activities against both B-Raf and EGFR kinases with IC_{50} values of 280 and 670 nM, and 3.90 and 1.92 μM, respectively. Further investigation revealed that the introduction of a 2-amino group (**5f**) in compound **5e** hardly affected its suppressing potency on B-Raf ^{V600E}, but the inhibitory effect on EGFR was significantly improved about 50-fold. The IC_{50} values of compound **5f** against B-Raf and EGFR were 410 and 43 nM, respectively, representing a new lead compound for further structural optimization. However, when a 6-hydroxyl group was introduced in compound **4**, the resulting compound **5g** totally failed to suppress the function of B-Raf. Its inhibitory potency on EGFR was also obviously decreased about 3-fold.

We further investigated the impact of the substituent on the 2-amino group on the B-Raf/EGFR dual inhibition by adopting compound **5f** as a new starting point. It was found that the compound is well tolerated to the N-substitution for the dual inhibition on B-Raf and EGFR. The *N*-methyl (**5h**), *N*-ethyl (**5i**), *N*-iropropyl (**5j**), *N*-cyclopropyl (**5k**), and *N*-cyclopentyl (**5l**) analogues displayed similar potencies on both B-Raf^{V600E} and EGFR to that of compound **5f**. Interestingly, although the *N*-phenyl compound **5n** showed an IC_{50} value of 210 nM on B-Raf ^{V600E} similar to that of **5f** (about 410 nM), its EGFR inhibitory effect is 10-fold more potent, and the IC_{50} value is about 6.0 nM. However, the *N*-cyclohexyl derivative (**5m**) showed about 8 times more improvement on the B-Raf suppressing effect, while its inhibitory activity on EGFR was almost identical to that of the lead compound **5f**. The IC_{50} values of compound **5m** on B-Raf^{V600E} and EGFR were 37 and 47 nM, respectively. Further investigation suggested that the N,N-disubstitution is detrimental to the compound's inhibitory activity on EGFR kinase, although it barely affects the inhibition on B-Raf. For instance, the *N*,*N*-dimethyl analogue (**5o**) displayed an IC_{50} value of 300 nM on B-Raf^{V600E}, which is almost identical to that of **5f**, but its IC_{50} value on EGFR is over 100 times greater than that of the lead compound, highlighting the critical role of a hydrogen bond donating moiety for the EGFR suppressing function.

Inspired by the above investigation, compounds containing either a pyrrolo[2,3-*b*]pyridinyl (**6a**) or 1*H*-pyrazolo[3,4-*b*]pyridinyl (**6b**) motif were designed by utilizing a conformation-constraining strategy. It was shown that both **6a** and **6b** displayed potencies against B-Raf^{V600E} similar to that of **5m**, with IC_{50} values of 51 and 48 nM, respectively, but their activities against EGFR differentiated obviously. Compound **6a** inhibited EGFR with an IC_{50} value of 8 nM, which is approximately 6-fold more potent than that of compound **5m**, while **6b** displayed an IC_{50} value of 30 nM, which is almost identical to that of **5m**. However, when a 1*H*-indol-5-yl group was introduced (**6c**), the resulting compound totally abolished its inhibitory effect on EGFR, and its potency on B-Raf^{V600E} was also decreased by a factor of 4. The strongly dual inhibition of compound **6a** against both EGFR and B-Raf ^{600E} makes it a highly promising lead compound for further investigation.

Further structural modification on **6a** suggested that the methyl group in ring B is optimal for the dual inhibition against B-Raf and EGFR. When the methyl was removed, although the resulting compound **6d** maintained a strong inhibition again B-Raf^{V600E} with an IC_{50} value of 48 nM, its potency on EGFR was dramaticly decreased about 90-fold. Whereas, the replacement of the methyl group with a relatively larger group, i.e., an ethyl

dx.doi.org/10.1021/jm500007h | J. Med. Chem. 2014, 57, 2692−2703

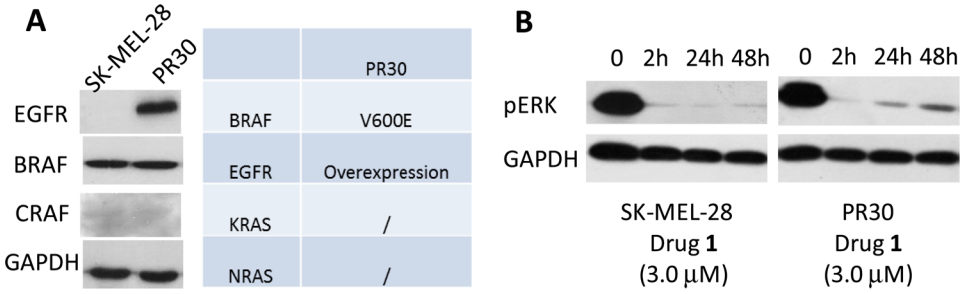

Figure 2. Clinical drug **1** potently and sustainably inhibits the activation of the MAPK path way in SK-MEL-28 melanoma cancer cells, but its effect on p-Erk is transient in the vemurafenib-resistant SK-MEL-28-PR30 cells. (A) The vemurafenib-induced resistant cancer cells harbor a high level of EGFR as determined by Western blot analysis but not k-Ras or n-Ras mutation. (B) Drug **1** potently and sustainably inhibits the activation of the MAPK path way in SK-MEL-28 melanoma cancer cells, but p-Erk reaccumulation was observed in the vemurafenib-resistant SK-MEL-28-PR30 cells after 24 h of treatment of **1**. Western blots were preformed after SK-MEL-28 and SK-MEL-28-PR30 cells were treated with drug **1** for the indicated time (2, 24, and 48 h).

Table 2. Compounds 6a and 6b Potently Inhibit the Proliferation of a Panel of Colorectal Cancer Cells Harboring Different States of EGFR and B-Raf Mutation

		Cell Growth Inhibition (IC_{50}, μM)[b]				
compds	cell lines	HT-29	COLO205	HCT116	LOVO	WiDr
	B-Raf	V600E	V600E	WT	WT	V600E
	EGFR[a]	++	+	++	−	+
6a		0.48 ± 0.04	0.22 ± 0.02	1.33 ± 0.07	0.17 ± 0.01	0.67 ± 0.14
6b		0.78 ± 0.03	0.36 ± 0.04	1.38 ± 0.19	0.48 ± 0.02	1.35 ± 0.07

[a]The level of EGFR were detected by immunoblotting (Supporting Information, Figure S1). [b]The antiproliferative activities of the compounds were evaluated using the MTS assay. Data are reported as the means ± SDs (standard deviations) from at least three independent experiments.

(**6e**) or an isopropyl (**6f**), induced a significant potency loss both on B-Raf and EGFR.

The antiproliferation effects of the new inhibitors against the vemurafenib-induced resistant SK-MEL-28-PR30 melanoma cancer cells (Supporting Information), which were demonstrated to harbor the B-Raf^{V600E} mutant and overexpression of EGFR (Figure 2A), together with the parental SK-MEL-28 cells with B-Raf^{V600E} mutation but low level of EGFR, were also investigated (Table 1). Highly consistent to the previous investigation, drug **1** potently inhibited the growth of the B-Raf^{V600E} mutated SK-MEL-28 cells with an IC_{50} value of 0.48 μM[41] but is almost totally inactive to suppress the proliferation of the PR30 cancer cells, which express high level of EGFR. Whereas, the selective EGFR inhibitor **3** did not show obvious growth inhibition on either SK-MEL-28-PR30 or SK-MEL-28 cells. Consistent with their weak dual inhibition against B-Raf ^{V600E} and EGFR, compounds **4** and **5a** only displayed minor suppressing effect on the growth of SK-MEL-28-PR30 and/or SK-MEL-28 cells. Not surprisingly, compounds **5b**, **5d**, **5e**, and **5g** are inactive to show an antiproliferative effect on the cancer cells, which might be a consequent effect of their poor inhibition against both B-Raf ^{V600E} and EGFR kinases. However, the dual inhibitor **5f** displayed moderate inhibition on both of the cancer cell lines with IC_{50} values of 1.84 and 1.89 μM. Other novel dual inhibitors, i.e., **5h**, **5i**, **5j**, **5k**, **5l**, **5m**, **5n**, **6d**, **6e**, and **6f**, also showed low micromolar values to suppress the growth of both vemurafenib-sensitive and vemurafenib-resistant melanoma cancer cells. Encouragingly, we were pleased to find that the two most potent B-Raf ^{V600E}/EGFR dual inhibitors, **6a** and **6b**, displayed the strongest inhibition against the cellular proliferation for both of the cancer cell lines. The compounds potently inhibited the growth of vemurafenib-sensitive SK-MEL-28 melanoma cancer cells with similar IC_{50} values to that of clinical drug **1**, which are 0.13, 0.54, and 0.48 μM. More significantly, they also displayed strong suppression on the proliferation of vemurafenib-resistant SK-MEL-28-PR30 cancer cells with IC_{50} values of 0.45 and 0.78 μM. It was also noteworthy that both of the compounds displayed almost identical potencies on the vemurafenib-sensitive and vemurafenib-resistant cancer cells, indicating their potential application to treat the intrinsic and acquired resistant melanoma and/or colorectal cancer cells with both B-Raf^{V600E} mutaition and EGFR overexpression.

Further investigation also revealed that the compounds indeed displayed strong inhibition against the growth of a panel of colorectal cancer cells harboring different states of EGFR and B-Raf mutation (Table 2). For instance, compound **6a** potently inhibited the growth of HT-29, COLO205, and WiDr colorectal cancer cells which carry the B-Raf ^{V600E} mutant and a high level of EGFR with IC_{50} values of 0.48, 0.22, and 0.67 μM, respectively. Interestingly, the compound also strongly suppressed the proliferation of HCT116 and LOVO colorectal cancer cells with IC_{50} values of 1.33 and 0.17 μM, respectively, although the cells harbor wild-type B-Raf.

The selectivity profile of **6a** against a panel of 456 kinases (including 395 different wild-type kinases) was also investigated by using the KINOMEscan platform (Ambit Bioscience, San Diego, USA) at a concentration of 1.0 μM, which was about 20−125 times its IC_{50} values against B-Raf^{V600E} and EGFR kinases, respectively. It was found that, in addition to its dual inhibition against EGFR and B-Raf^{V600E}, compound **6a** also exhibited strong suppression on ERRB2, ERRB4, and PDGFRβ kinases, which have been demonstrated to indirectly mediate (i.e., ERRB2 through ERRB3[34]) or directly link (PDGFRβ[23]) with the acquired resistance of melanoma. However, special attention is also required to further investigate the potential

dx.doi.org/10.1021/jm500007h | J. Med. Chem. 2014, 57, 2692−2703

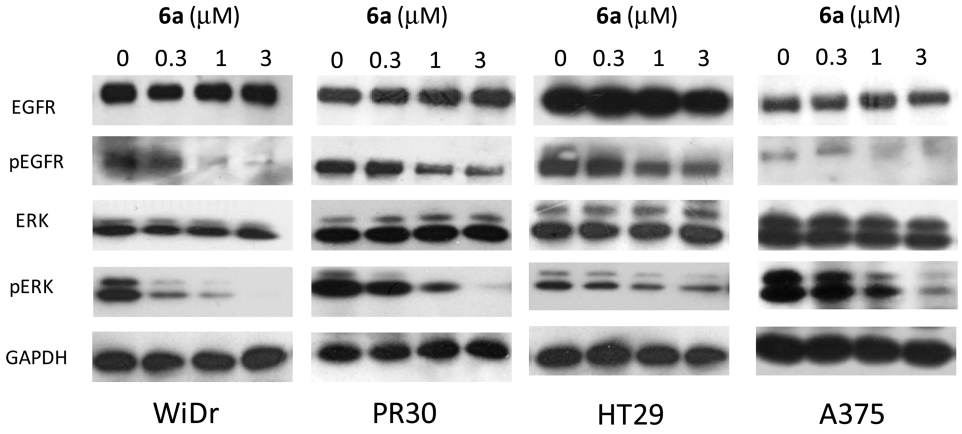

Figure 3. Inhibitor **6a** dose-dependenty inhibits the activation of the MAPK path way and the phosphorylation of EGFR in SK-MEL-28 PR30, A375 melanoma cancer cells, and WiDr, HT29 colorectal cancer cells. Western blots were performed after the cells were treated with **6a** for 2.0 h.

safety issue of **6a** associated with its relatively broad inhibition on a panel of other kinases (Supporting Information).

In order to further validate the dual inhibitory effects of new inhibitors, we investigated their suppressive functions on the activation of the MAPK signal pathway and the phosporylation of EGFR protein in self-constructed SK-MEL-28-PR30 cells which have been demonstrated to harbor B-Raf^{V600E} mutation and EGFR amplification (Figure 2A) by taking compound **6a** as an example. As shown in Figure 3, the treatment of compound **6a** indeed caused a dose-dependent reduction of the phosphorylation of Erk in SK-MEL-28-PR30 cells, indicating the blockage of the MAPK signal pathway. Furthermore, the activation of EGFR was also obviously inhibited by **6a**, while the total protein levels of EGFR, Erk, and GAPDH remained unchanged. Further investigation demonstrated that the compound also potently blocked the MAPK signal pathway and suppressed the activation of EGFR in WiDr, HT29 colorectal cancer cells, and A375 melanoma cancer cells which express a relatively high level of EGFR and B-Raf^{V600E} mutation.

Similar to the previous data obtained from WiDr colorectal cancer cell models,[25] our investigation also demonstrated that although drug **1** induced highly potent and sustainable suppression on the activation of MAPK signal pathway in vemurafenib-sensitive SK-MEL-28 melanoma cancer cells, its effect on p-Erk is transient, and significant reaccumulation of p-Erk could be observed in the vemurafenib-resistant SK-MEL-28-PR30 cells after 24 h (Figures 2B and 4). The unsustainable inhibition on the MAPK pathway may contribute greatly to the intrinsic and acquired insensitivity of B-Raf mutated melanoma

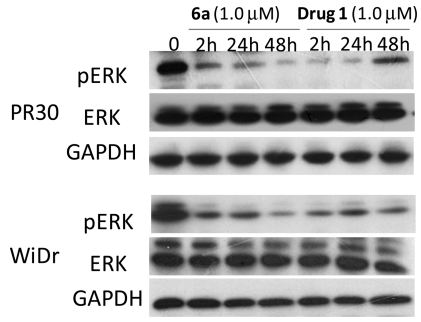

Figure 4. Inhibitor **6a** potently and sustainably inhibits the activation of the MAPK path way in SK-MEL-28 PR30 melanoma cancer cells and WiDr colorectal cancer cells.

and/or colorectal cancer cells to drug **1**. In order to get a better understanding on the strong inhibition of **6a** against the proliferation of vemurafenib-resistant SK-MEL-28-PR 30 cells, we also investigated the suppressing effect of this compound on the activation of p-Erk at different time courses. It was shown that compound **6a** sustainably inhibited the phosphorylation of Erk at a concentration of 1.0 μM and that p-Erk suppression was successfully maintained after 48-h treatments. As a parallel comparison, drug **1** only displayed a transient inhibition on the phosphorylation of Erk at 1.0 μM, and the p-Erk was significantly reaccumulated in 48 h, which may be due to a consequent upregulation of erbB3 by the transphosphorylation partner EGFR.[34] A similar sustainable inhibition of p-Erk by **6a** was also observed in WiDr colorectal cancer cells. These results strongly support the potential of these compounds to overcome the intrinsic and acquired resistant melanoma and/or colorectal cancer cells with EGFR overexpression.

In summary, a series of 1*H*-pyrazolo[3,4-*b*]pyridine-5-carboxamide analogues were identified as novel dual inhibitors of the EGFR and B-Raf^{V600E} mutant. The compounds potently inhibited both of the kinases with low nanomolar IC_{50} values and strongly suppressed the proliferation of a panel of intrinsic and acquired resistant melanoma and/or colorectal cancer cells harboring overexpressed EGFR with submicromolar IC_{50} values. Furthermore, the representative compounds **6a** also displayed potent and sustainable inhibition against the activation of the MAPK path way in the resistant SK-MEL-28 PR30 melanoma cancer cells and WiDr colorectal cancer cells, suggesting that the EGFR/B-Raf^{V600E} dual inhibition, at least in part, might be a tractable strategy to overcome the intrinsic and acquired resistance of melanoma and/or colorectal cancers against the current B-Raf^{V600E} inhibitor therapy. Further structural optimization to improve pharmacokinetic properties, *in vivo* pharmacodynamic evaluation, and molecular mechanism studies on this class of compounds are in progress and will be reported in due course. However, it is also noteworthy that EGFR amplification is not the only key player for the intrinsic and acquired resistance of melanoma and/or colorectal cancer cells against current B-Raf inhibitors. New medicinal chemistry efforts based on an understanding of the extensive mechanism will be highly worthwhile for overcoming the resistance.

EXPERIMENTAL SECTION

General Methods for Chemistry. All reagents and solvents were used directly as purchased from commercial sources. Flash

dx.doi.org/10.1021/jm500007h | J. Med. Chem. 2014, 57, 2692−2703

chromatography was performed using silica gel (300 mesh). All reactions were monitored by TLC, using silica gel plates with fluorescence F_{254} and UV light visualization. ^{1}H NMR and ^{13}C NMR spectra were recorded on a Bruker AV-400 spectrometer at 400 MHz and a Bruker AV-500 spectrometer at 125 MHz. Coupling constants (J) are expressed in hertz (Hz). Chemical shifts (δ) of NMR are reported in parts per million (ppm) units relative to an internal control (TMS). Low resolution ESI-MS were recorded on an Agilent 1200 HPLC-MSD mass spectrometer and high resolution ESI-MS on an Applied Biosystems Q-STAR Elite ESI-LC-MS/MS mass spectrometer. The purity of compounds was determined by reverse-phase high performance liquid chromatography (HPLC) analysis to be >95%. HPLC instrument, Dionex Summit HPLC (column, Diamonsil C18, 5.0 μm, 4.6 × 250 mm (Dikma Technologies); detector, PDA-100 photodiode array; injector, ASI-100 autoinjector; pump, p-680A). A flow rate of 1.0 mL/min was used with a mobile phase of MeOH in H_2O with a 0.1% modifier (ammonia or trifluoroacetate, v/v).

4-Methyl-*N*-(4-((4-methylpiperazin-1-yl)methyl)-3-(trifluoromethyl)phenyl)-3-nitrobenzamide 9a. 4-((4-Methylpiperazin-1-yl)methyl)-3-(trifluoromethyl)aniline **7** (7.97g, 44.0 mmol) and 4-methyl-3-nitrobenzoic acid **8a** (10.00g, 36.6 mmol) were stirred in 20 mL of dry tetrahydrofuran (THF) at room temperature. To the mixture, PyBOP (28.60g, 54.9 mmol) and triethylamine (8.2 mL, 58.56 mmol) were added. The resulting mixture was stirred at room temperature overnight, and then the organic solvent was removed under vacuum. The resulting residue was diluted with water and extracted with ethyl acetate (2 × 50 mL). The combined organic layer was dried over anhydrous sodium sulfate and concentrated under vacuum and then purified by column chromatography over silica gel to afford pure compound **9a** (7.50g, yield: 50%). ^{1}H NMR (400 MHz, $CDCl_3$) δ 9.61 (s, 1 H), 8.53 (d, J = 1.6 Hz, 1 H), 8.14 (dd, J = 9.6 Hz, 1.6 Hz, 1 H), 8.10 (d, J = 2.0 Hz, 1 H), 7.81 (dd, J = 8.4 Hz, 1.6 Hz, 1 H), 7.91 (d, J = 8.4 Hz, 1 H), 7.41 (d, J = 8.0 Hz, 1 H), 3.62 (s, 2 H), 3.31−2.23(m, 8 H), 2.83 (s, 3 H), 2.59 (s, 3 H). Compounds **9b−d** were synthesized by using a similar procedure; yield, 46−85%.

3-Amino-4-methyl-*N*-(4-((4-methylpiperazin-1-yl)methyl)-3-(trifluoromethyl)phenyl) benzamide 10a. To a solution of **9a** (7.50g, 17.2 mmol) in 30 mL of methanol, 0.75g Pd/C was added, and the reaction flask was evacuated and backfilled with hydrogen twice. The reaction mixture was stirred at room temperature under a hydrogen balloon for 5 h. The reaction mixture was filtered through a pad of Celite and concentrated under vacuum to yield **10a** (5.20g, yield: 75%). ^{1}H NMR (400 MHz, DMSO-d_6) δ 10.27 (s, 1 H), 8.22 (d, J = 2.0 Hz, 1 H), 8.04 (dd, J = 8.4 Hz, 1.6 Hz, 1 H), 7.66 (d, J = 8.4 Hz, 1 H), 7.22 (d, J = 1.6 Hz, 1 H), 7.13−7.06 (m, 2 H), 5.08 (s, 2 H), 3.54 (s, 2 H), 3.41 (s, 1 H), 2.48−2.21 (m, 7 H), 2.13 (m, 6 H). Compounds **10b−d** were synthesized by using a similar procedure; yield, 68−92%.

3-Amino-4-ethyl-*N*-(4-((4-methylpiperazin-1-yl)methyl)-3-(trifluoromethyl)phenyl)benzamide 10c. ^{1}H NMR (500 MHz, DMSO-d_6) δ 10.29 (s, 1H), 8.21 (d, J = 1 Hz, 1H), 8.05 (d, J = 8.5 Hz, 1H), 7.67 (d, J = 8.5 Hz, 1H), 7.16 (s, 1H), 7.11 (d, J = 8.0 Hz, 1H), 7.06 (d, J = 8.0 Hz, 1H), 5.12 (s, 2H), 3.61 (s, 2H), 2.84 −2.49 (m, 8H), 2.51 (q, J = 7.5 Hz, 2H), 1.15 (t, J = 7.5 Hz, 3H); ^{13}C NMR (125 MHz, DMSO-d_6) δ 166.99, 147.41, 146.48, 139.19, 133.27, 131.73, 131.28, 131.18, 128.22, 123.67, 117.51, 115.65, 113.92, 60.15, 57.35, 54.07 (2C), 51.21, 44.07, 23.84, 13.35; MS (ESI), m/z 421 $[M + H]^+$.

***N*-(2-Methyl-5-((4-((4-methylpiperazin-1-yl)methyl)-3-(trifluoromethyl)phenyl)carbamoyl) phenyl)nicotinamide 4.** To a solution of **10a** (100.0 mg, 0.25 mmol) in 5 mL of *N*,*N*-dimethylformamide (DMF), 46.4 mg of nicotinic acid (0.38 mmol), (1-[bis(dimethylamino) methylene]-1*H*-1,2,3-triazolo[4,5-*b*]-pyridinium 3-oxid hexafluorophosphate) (HATU) (140.1 mg, 0.37 mmol), and *N*,*N*-diisopropylethylamine (DIPEA) (0.13 mL, 0.75 mmol) were added. The resulting mixture was stirred at room temperature overnight. The reaction was quenched with water and extracted with ethyl acetate (3 × 20 mL). The combined organic layer was dried over anhydrous sodium sulfate, concentrated under vacuum, and then purified by column chromatography over silica gel to afford pure compound **4** (72.9 mg) (yield: 57%). ^{1}H NMR (400 MHz, DMSO-d_6) δ 10.47 (s, 1 H), 10.27 (s, 1 H), 9.17 (s, 1 H), 8.79 (d, J = 3.6 Hz, 1 H), 8.34 (d, J = 7.6 Hz, 1 H), 8.20 (s, 1 H), 8.06 (d, J = 8.0 Hz, 1 H), 8.01 (s, 1 H), 7.85 (d, J = 8.0 Hz, 1 H), 7.70 (d, J = 4.4 Hz, 1 H), 7.60 (dd, J = 4.8 Hz, 7.6 Hz, 1 H), 7.48 (d, J = 8.0 Hz, 1 H), 3.56 (s, 2H), 2.40−2. 32 (m, 11 H), 2.16 (s, 3 H). ^{13}C NMR (125 MHz, DMSO-d_6) δ 165.10, 164.19, 152.30, 148.70, 138.27, 138.23, 136.17, 135.50, 132.37, 132.03, 131.27, 130.55, 129.94, 127.54, 126.02, 125.51, 123.65, 123.57, 117.38, 117.30, 57.45, 54.68(2C), 52.62(2C), 45.63, 18.00. HRMS (ESI) calcd for $C_{27}H_{28}F_3N_5O_2$ $[M + H]^+$, 512.2268; found, 512.2272. HPLC purity = 97.06%, Rt 5.82 min.

Compounds **5a−o** and **6a−f** were synthesized by using a similar procedure.

***N*-(2-Methyl-5-((4-((4-methylpiperazin-1-yl)methyl)-3-(trifluoromethyl)phenyl) carbamoyl) phenyl)picolinamide 5a.** Yield: 52%. ^{1}H NMR (400 MHz, DMSO-d_6) δ 10.47 (s, 1 H), 10.27 (s, 1 H), 9.17 (d, J = 1.5 Hz, 1 H), 8.79 (dd, J = 4.8, 1.5 Hz, 1 H), 8.34 (d, J = 8.0 Hz, 1 H), 8.20 (d, J = 1.8 Hz, 1 H), 8.07 (d, J = 8.4 Hz, 1 H), 8.01 (s, 1 H), 7.85 (dd, J = 8.0 Hz, 1.5 Hz, 1 H), 7.70 (d, J = 8.5 Hz, 1 H), 7.60 (dd, J = 7.7 Hz, 4.8 Hz, 1 H), 7.48 (d, J = 8.1 Hz, 1 H), 3.56 (s, 2 H), 2.39−2.33 (m, 11 H), 2.18 (s, 3 H). ^{13}C NMR (125 MHz, DMSO-d_6) δ 165.16, 164.25, 152.34, 148.72, 138.32, 138.26, 136.20, 135.55, 132.40, 132.04, 131.32, 130.61, 129.97, 126.05, 125.56, 123.71(2C), 123.62, 117.19, 117.08, 57.45, 54.66(2C), 52.55(2C), 45.56, 18.03. HRMS (ESI) calcd for $C_{27}H_{28}F_3N_5O_2$ $[M + H]^+$, 512.2268; found, 512.2266. HPLC purity = 95.01%, Rt 6.16 min.

***N*-(2-Methyl-5-((4-((4-methylpiperazin-1-yl)methyl)-3-(trifluoromethyl)phenyl) carbamoyl) phenyl)isonicotinamide 5b.** Yield: 61%. ^{1}H NMR (400 MHz, DMSO-d_6) δ 10.46 (s, 1 H), 10.34 (s, 1 H), 8.81 (dd, J = 4.4 Hz, 1.6 Hz, 2 H), 8.20 (d, J = 2.0 Hz, 1 H), 8.07 (dd, J = 8.8 Hz, 1.8 Hz, 1 H), 8.01 (d, J = 1.2 Hz, 1 H), 7.92−7.90 (m, 2 H), 7.86 (dd, J = 8.0 Hz, 1.8 Hz, 1 H), 7.70 (d, J = 8.8 Hz, 1 H), 7.47 (d, J = 8.0 Hz, 1 H), 3.56 (s, 2 H), 2.50−2.33 (m, 11 H), 2.16 (s, 3 H). ^{13}C NMR (125 MHz, DMSO-d_6) δ 164.96, 164.03, 150.35(2C), 141.25, 138.22, 135.93, 132.36, 131.97, 131.17, 130.50, 127,48, 127.25, 126.00, 125.62, 123.49, 121.53(2C), 117.28, 117.23, 57.41, 54.67(2C), 52.62(2C), 45.63, 17.91. HRMS (ESI) calcd for $C_{27}H_{28}F_3N_5O_2$ $[M + H]^+$, 512.2268; found, 512.2269. HPLC purity = 97.9%, Rt 5.82 min.

3-Benzamido-4-methyl-*N*-(4-((4-methylpiperazin-1-yl)-methyl)-3-(trifluoromethyl) phenyl) benzamide 5c. Yield: 65%. ^{1}H NMR (400 MHz, DMSO-d_6) δ 10.48 (s, 1 H), 10.08 (s, 1 H), 8.21 (s, 1 H), 8.7 (d, J = 8.5 Hz, 1 H), 8.03 (s, 1 H), 8.01 (s, 2 H), 7.83 (d, J = 8 Hz, 1 H), 7.70 (d, J = 8.5 Hz, 1 H), 7.63−7.53 (m, 3 H), 7.46 (d, J = 8.0 Hz, 1 H), 3.56 (s, 2 H), 2.50−2.31 (m, 11 H), 2.15 (s, 3 H). ^{13}C NMR (125 MHz, DMSO-d_6) δ 165.46, 165.06, 138.23, 136.58, 134.25, 132.25, 131.93, 131.63, 131.16, 130.37, 128.42, 127.61, 127.47, 127.23, 126.02, 125.40, 125.23, 123.48, 123.22, 117.26, 117.21, 57.41, 54.67(2C), 52.64(2C), 45.64, 17.96. HRMS (ESI) calcd for $C_{28}H_{29}F_3N_4O_2$ $[M + H]^+$, 511.2316; found, 511.2314. HPLC purity = 98.6%, Rt 7.23 min.

***N*-(2-Methyl-5-((4-((4-methylpiperazin-1-yl)methyl)-3-(trifluoromethyl)phenyl) carbamoyl) phenyl)pyrazine-2-carboxamide 5d.** Yield: 47%. ^{1}H NMR (400 MHz, DMSO-d_6) δ 10.48 (s, 2 H), 9.33 (s, 1 H), 8.97 (d, J = 2.3 Hz, 1 H), 8.85 (s, 1 H), 8.24 (s, 1 H), 8.20 (s, 1 H), 8.07 (d, J = 8.5 Hz, 1 H), 7.83 (d, J = 7.9 Hz, 1 H), 7.70 (d, J = 8.0 Hz, 1 H), 7.47 (d, J = 8.0 Hz, 1 H), 3.56 (s, 2 H), 2.48−2.25 (m, 11 H), 2.17 (s, 3 H). ^{13}C NMR (125 MHz, DMSO-d_6) δ 165.23, 161.80, 148.03, 144.62, 143.92, 143.52, 138.27, 136.77, 135.84, 132.53, 132.02, 131.30, 130.50, 127.58, 125.47, 125.13, 124.54, 123.59, 117.32, 57.46, 54.67(2C), 52.57(2C), 45.59, 17.78. HRMS (ESI) calcd for $C_{26}H_{27}F_3N_6O_2$ $[M + H]^+$, 513.2221; found, 513.2228. HPLC purity = 99.64%, Rt 7.01 min.

***N*-(2-Methyl-5-((4-((4-methylpiperazin-1-yl)methyl)-3-(trifluoromethyl)phenyl) carbamoyl) phenyl)pyrimidine-5-carboxamid 5e.** Yield: 45%. ^{1}H NMR (400 MHz, DMSO-d_6) δ 10.48(s, 1 H), 10.42 (s, 1 H), 9.40 (s, 1 H), 9.32 (s, 2 H), 8.20 (s, 1 H), 8.19−8.03 (m, 2 H), 7.86 (dd, J = 8.0 Hz, 1.8 Hz, 1 H), 7.70 (d, J = 8.4 Hz, 1 H), 7.48 (d, J = 8.0 Hz, 1 H), 3.56 (s, 2 H), 2.39−2.35 (m, 11 H), 2.15 (s, 3 H). ^{13}C NMR (125 MHz, DMSO-d_6) δ 164.98, 162.34, 160.27, 156.23(2C), 138.18, 138.00, 135.74, 132.40, 131.99, 131.19, 130.54, 127.96, 127.24, 125.81, 125.54, 123.50, 117.28, 117.23, 57.42,

54.68(2C), 52.65(2C), 45.66, 17.96. HRMS (ESI) calcd for $C_{26}H_{27}F_3N_6O_2$ $[M + H]^+$, 513.2221; found, 513.2229. HPLC purity = 98.70%, Rt 5.90 min.

2-Amino-*N*-(2-methyl-5-((4-((4-methylpiperazin-1-yl)-methyl)-3-(trifluoromethyl) phenyl) carbamoyl)phenyl)-pyrimidine-5-carboxamide 5f. Yield: 38%. ^{1}H NMR (400 MHz, DMSO-d_6) δ 10.47 (s, 1 H), 9.88 (s, 1 H), 8.83 (s, 2 H), 8.20 (s, 1 H), 8.06 (d, J = 8.4 Hz, 1 H), 7.98 (s, 1 H), 7.81 (d, J = 7.6 Hz, 1 H), 7.69 (d, J = 8.4 Hz, 1 H), 7.44 (d, J = 8.0 Hz,1 H) 7.34 (s, 2 H), 3.56 (s, 2 H), 2.49−2.30 (m, 11 H), 2.20 (s, 3 H). ^{13}C NMR (125 MHz, DMSO-d_6) δ 165.73, 164.74, 163.64, 158.81(2C), 138.67, 138.50, 136.61, 132.59, 132.35, 131.73, 128.00, 127.77, 126.29, 125.76, 125.64, 124.02, 123.58, 117.79, 116.69, 57.69, 54.78(2C), 52.57(2C), 45.59, 18.33; HRMS (ESI) calcd for $C_{26}H_{28}F_3N_7O_2$ $[M + H]^+$, 528.2330; found, 528.2332. HPLC purity = 97.80%, Rt 5.15 min.

6-Hydroxy-*N*-(2-methyl-5-((4-((4-methylpiperazin-1-yl)-methyl)-3-(trifluoromethyl)phenyl) carbamoyl) phenyl)-nicotinamide 5g. Yield: 56%. ^{1}H NMR (400 MHz, DMSO-d_6) δ 12.10 (s, 1 H), 10.47 (s, 1 H), 9.82 (s, 1 H), 8.21−8.19 (m, 2 H), 8.11 (d, J = 8.4 Hz, 1 H), 7.97 (dd, J = 9.6, 2.8 Hz, 1 H), 7.94 (d, J = 1.6 Hz, 1 H), 7.81 (dd, J = 8.0, 1.6 Hz, 1 H), 7.70 (d, J = 8.8 Hz, 1 H), 7.44 (d, J = 8.4 Hz, 1 H), 6.43 (d, J = 9.6 Hz, 1 H), 3.65 (s, 2 H), 3.30−2.50 (br, 8 H), 2.73 (s, 3 H), 2.29 (s, 3 H). ^{13}C NMR (125 MHz, DMSO-d_6) δ 165.49, 163.15, 162.77, 139.61, 138.65, 138.58, 138.55, 136.85, 132.66, 132.38, 131.61, 130.81, 127.91, 127.67, 126.40, 125.85, 125.55, 123.92, 123.67, 119.45, 117.65, 112.49, 57.87, 55.13(2C), 53.10(2C), 46.12, 18.43; HRMS (ESI) calcd for $C_{27}H_{28}F_3N_5O_3$ $[M + H]^+$, 528.2217; found, 528.2220. HPLC purity = 97.72%, Rt 4.43 min.

***N*-(2-Methyl-5-((4-((4-methylpiperazin-1-yl)methyl)-3-(trifluoromethyl)phenyl)carbamoyl) phenyl)-2-(methylamino)-pyrimidine-5-carboxamide 5h.** Yield: 55%. ^{1}H NMR (400 MHz, DMSO-d_6) δ 10.45 (s, 1 H), 9.86 (s, 1 H), 8.90 (s, 1 H), 8.83 (s, 1 H), 8.20 (s, 1 H), 8.06 (d, J = 8.4 Hz, 1 H), 7.99 (s, 1 H), 7.82−7.80 (m, 2 H), 7.70 (d, J = 8.5 Hz, 1 H), 7.44 (d, J = 7.9 Hz, 1 H), 3.56 (s, 2 H), 2.88 (d, J = 4.6 Hz, 3 H), 2.39−2.30 (m, 11 H), 2.16 (s, 3 H). ^{13}C NMR (125 MHz, DMSO-d_6) δ 165.06, 163.34, 162.98, 158.13 (2C), 138.21, 138.05, 136.37, 132.21, 131.92, 131.17, 130.39, 127.38, 125.84, 125.11, 123.48, 117.25, 117.21, 115.85, 57.40, 54.67 (2C), 52.62 (2C), 45.63, 27.86, 18.01. HRMS (ESI) calcd for $C_{27}H_{30}F_3N_7O_2$ $[M + H]^+$, 542.2486; found, 542.2486. HPLC purity = 95.62%, Rt 6.35 min.

2-(Ethylamino)-*N*-(2-methyl-5-((4-((4-methylpiperazin-1-yl)-methyl)-3-(trifluoromethyl)phenyl) carbamoyl)phenyl)-pyrimidine-5-carboxamide 5i. Yield: 30%. ^{1}H NMR (400 MHz, DMSO-d_6) δ 10.46 (s, 1 H), 9.85 (s, 1 H), 8.88 (s, 1 H), 8.83 (s, 1 H), 8.20 (s, 1 H), 8.07 (d, J = 8.1 Hz, 1 H), 7.98 (s, 1 H), 7.89 (t, J = 5.7 Hz, 1 H), 7.81 (d, J = 7.9 Hz, 1 H), 7.73−7. 65 (m, 2 H), 7.44 (d, J = 8.1 Hz, 1 H), 3.57 (s, 2 H), 3.38 (q, J = 7.0 Hz, 2 H), 2.40 (s, 7 H), 2.31 (s, 4 H), 2.20 (s, 3 H), 1.15 (t, J = 7.1 Hz, 3 H). ^{13}C NMR (125 MHz, DMSO-d_6) δ 167.02, 165.21, 163.13, 162.84, 158.24, 138.29, 138.15, 136.44, 132.28, 131.94, 131.30, 130.49, 128.69, 125.92, 125.18, 123.59, 123.29, 117.33, 115.91, 57.41, 54.58(2C), 52.41(2C), 45.42, 35.60, 18.06, 14.51. HRMS (ESI) calcd for $C_{28}H_{32}F_3N_7O_2$ $[M + H]^+$, 556.2643; found, 556.2644. HPLC purity = 99.38%, Rt 6.73 min.

2-(Isopropylamino)-*N*-(2-methyl-5-((4-((4-methylpiperazin-1-yl)methyl)-3-(trifluoromethyl) phenyl)carbamoyl)phenyl)-pyrimidine-5-carboxamide 5j. Yield: 52%. ^{1}H NMR (400 MHz, DMSO-d_6) δ 10.46 (s, 1 H), 9.84 (s, 1 H), 8.84 (s, 2 H), 8.20 (s, 1 H), 8.06 (d, J = 8.2 Hz, 1 H), 7.98 (s, 1 H), 7.80 (t, J = 7.8 Hz, 2 H), 7.70 (d, J = 8.5 Hz, 1 H), 7.44 (d, J = 7.8 Hz, 1 H), 4.17−4.11 (m, 1 H), 3.56 (s, 2 H), 2.41−2. 30 (m, 11 H), 2.16 (s, 3 H), 1.18 (d, J = 6.3 Hz, 6 H). ^{13}C NMR (125 MHz, DMSO-d_6) δ 165.07, 162.97, 162.19, 158.16, 158.14, 138.22, 138.01, 136.40, 132.22, 131.92, 131.17, 130.37, 125.82, 125.05, 123.48, 123.22, 117.25, 117.20, 115.72, 57.41, 54.66 (2C), 52.61 (2C), 45.63, 42.25, 22.13 (2C), 18.00. HRMS (ESI) calcd for $C_{29}H_{34}F_3N_7O_2$ $[M + H]^+$, 570.2799; found, 570.2798. HPLC purity = 98.64%, Rt 7.63 min.

2-(Cyclopropylamino)-*N*-(2-methyl-5-((4-((4-methylpiperazin-1-yl)methyl)-3-(trifluoromethyl) phenyl)carbamoyl)-phenyl)pyrimidine-5-carboxamide 5k. Yield: 48%. ^{1}H NMR (400 MHz, DMSO-d_6) δ 10.46 (s, 1 H), 9.88 (s, 1 H), 8.88 (s, 2 H), 8.20 (d, J = 2.0 Hz, 1 H), 8.08−8.04 (m, 2 H), 7.99 (d, J = 1.6 Hz, 1 H), 7.82 (dd, J = 7.9, 1.6 Hz, 1 H), 7.70 (d, J = 8.6 Hz, 1 H), 7.45 (d, J = 8.1 Hz, 1 H), 3.56 (s, 2 H), 2.82 (tq, J = 7.5, 3.9 Hz, 1 H), 2.40−2.31 (m, 11 H), 2.15 (s, 3 H), 0.75−0.70 (m, 2 H), 0.55−0.51 (m, 2 H). ^{13}C NMR (125 MHz, DMSO-d_6) δ 165.06, 164.03, 162.96, 158.05, 158.03, 138.21, 138.01, 136.36, 132.23, 131.93, 131.17, 130.38, 125.81, 125.09, 123.48, 117.26, 117.21, 116.50, 57.41, 54.68 (2C), 52.65 (2C), 45.66, 23.95, 17.99, 6.24 (2C). HRMS (ESI) calcd for $C_{29}H_{32}F_3N_7O_2$ $[M + H]^+$, 528.2643; found, 528.2640. HPLC purity = 96.68%, Rt 6.80 min.

2-(Cyclopentylamino)-*N*-(2-methyl-5-((4-((4-methylpiperazin-1-yl)methyl)-3-(trifluoromethyl) phenyl)carbamoyl)-phenyl)pyrimidine-5-carboxamide 5l. Yield: 52%. ^{1}H NMR (400 MHz, DMSO-d_6) δ 10.45 (s, 1 H), 9.84 (s, 1 H), 8.85 (s, 2 H), 8.20 (s, 1 H), 8.06 (d, J = 8.0 Hz, 1 H), 7.99 (s, 1 H), 7.90 (d, J = 7.2 Hz, 1 H), 7.81 (d, J = 7.6 Hz, 1 H), 7.69 (d, J = 8.4 Hz, 1 H), 7.43 (d, J = 8.0 Hz, 1 H), 4.27 (t, J = 6.6 Hz, 1 H), 3.56 (s, 2 H), 2.50−2.31 (m, 11 H), 2.18 (s, 3 H), 1.92 (d, J = 3.6 Hz, 2 H), 1.70 (s, 2 H), 1.54 (s, 4 H). ^{13}C NMR (125 MHz, DMSO-d_6) δ 165.09, 163.01, 162.56, 158.08, 138.24, 138.02, 136.41, 132.23, 131.88, 131.17, 130.36, 127.48, 125.84, 125.06, 123.48, 123.22, 117.26, 117.22, 115.75, 57.39, 54.61(2C), 52.53(2C), 52.34, 45.53, 32.04(2C), 23.38(2C), 18.00. HRMS (ESI) calcd for $C_{31}H_{36}F_3N_7O_2$ $[M + H]^+$, 596.2956; found, 596.2959. HPLC purity = 96.00%, Rt 9.32 min.

2-(Cyclohexylamino)-*N*-(2-methyl-5-((4-((4-methylpiperazin-1-yl)methyl)-3-(trifluoromethyl) phenyl)carbamoyl)phenyl)-pyrimidine-5-carboxamide 5m. Yield: 66%. ^{1}H NMR (400 MHz, DMSO-d_6) δ 10.45 (s, 1 H), 9.83 (s, 1 H), 8.84 (s, 2 H), 8.20 (d, J = 1.8 Hz, 1 H), 8.06 (d, J = 8.4 Hz, 1 H), 7.99 (d, J = 1.2 Hz, 1 H), 7.82 (s, 1 H), 7.80 (s, 1 H), 7.70 (d, J = 8.6 Hz, 1 H), 7.44 (d, J = 8.1 Hz, 1 H), 3.82−3.79 (m, 1 H), 3.56 (s, 2 H), 2.47−2. 30 (m, 11 H), 2.15 (s, 3 H), 1.89 (s, 2 H), 1.73 (s, 2 H), 1.60 (d, J = 12.0 Hz, 1 H), 1.30 (dd, J = 16.0, 7.9 Hz, 4 H), 1.18−1.12 (m, 1 H). ^{13}C NMR (125 MHz, DMSO-d_6) δ 165.06, 162.95, 162.19, 158.17, 138.20, 137.99, 136.39, 132.21, 131.92, 131.16, 130.36, 127.22, 125.80, 125.39, 125.05, 123.47, 117.25, 117.20, 115.72, 57.41, 54.68 (2C), 52.65 (2C), 49.45, 45.66, 32.17 (2C), 25.23, 24.68 (2C), 17.98. HRMS (ESI) calcd for $C_{32}H_{38}F_3N_7O_2$ $[M + H]^+$, 610.3112; found, 610.3114. HPLC purity = 99.42%, Rt 11.84 min.

***N*-(2-Methyl-5-((4-((4-methylpiperazin-1-yl)methyl)-3-(trifluoromethyl)phenyl)carbamoyl) phenyl)-2-(phenylamino)-pyrimidine-5-carboxamide 5n.** Yield: 81%, ^{1}H NMR (400 MHz, DMSO-d_6) δ 10.48 (s, 1 H), 10.20 (s, 1 H), 10.04 (s, 1 H), 9.04 (s, 2 H), 8.20 (s, 1 H), 8.05−8.02 (m, 2 H), 7.80−7.78 (m, 3 H), 7.71 (s, 1 H), 7.46 (d, J = 6.4 Hz, 1 H), 7.34 (s, 2 H), 7.03 (s, 1 H), 3.56 (s, 2 H), 2.49−2.33 (m, 11 H), 2.18 (s, 3 H). ^{13}C NMR (125 MHz, DMSO-d_6) δ 165.61, 163.17, 161.27, 158.48(2C), 139.84, 138.58, 138.55, 136.58, 132.68, 132.37, 131.69, 130.95, 129.02(2C), 126.26, 125.70, 123.99, 123.02, 120.21(2C), 118.69, 117.71, 57.77, 54.93(2C), 52.78(2C), 45.79, 18.40; HRMS (ESI) calcd for $C_{32}H_{32}F_3N_7O_2$ $[M + H]^+$, 604.2643; found, 604.2642. HPLC purity = 99.42%, Rt 8.29 min.

2-(Dimethylamino)-*N*-(2-methyl-5-((4-((4-methylpiperazin-1-yl)methyl)-3-(trifluoromethyl) phenyl)carbamoyl)phenyl)-pyrimidine-5-carboxamide 5o. Yield: 71%. ^{1}H NMR (400 MHz, DMSO-d_6) δ 10.47 (s, 1 H), 9.90 (s, 1 H), 8.91 (s, 2 H), 8.20 (s, 1 H), 8.06 (d, J = 7.6 Hz, 1 H), 7.99 (s, 1 H), 7.81 (d, J = 7.6 Hz, 1 H), 7.69 (d, J = 7.6 Hz, 1 H), 7.40 (d, J = 7.6 Hz, 1 H), 3.56 (s, 2 H), 3.21 (s, 6 H), 2.50−2.31 (m, 11 H), 2.19 (s, 3 H). ^{13}C NMR (125 MHz, DMSO-d_6) δ 165.63, 163.58, 162.54(2C), 138.58, 136.69, 132.62, 132.29, 131.70, 130.91, 126.27, 125.61, 123.98, 117.72, 115.47, 57.72, 54.83(2C), 52.61(2C), 45.61, 37.21(2C), 18.37; HRMS (ESI) calcd for $C_{28}H_{32}F_3N_7O_2$ $[M + H]^+$, 556.2643; found, 556.2641. HPLC purity = 97.80%, Rt 7.51 min.

***N*-(2-Methyl-5-((4-((4-methylpiperazin-1-yl)methyl)-3-(trifluoromethyl)phenyl)carbamoyl) phenyl)-1*H*-pyrrolo[2,3-b]pyridine-5-carboxamide 6a.** Yield: 63%. ^{1}H NMR (400 MHz, DMSO-d_6) δ 11.99 (s, 1 H), 10.47 (s, 1 H), 10.09 (s, 1 H), 8.88 (d, J = 2.4 Hz, 1 H), 8.61 (d, J = 1.6 Hz, 1 H), 8.21 (d, J = 2.0 Hz, 1 H), 8.07 (d, J = 8.4 Hz, 1 H), 8.04 (d, J = 1.3 Hz, 1 H), 7.83 (dd, J = 7.9, 1.6 Hz, 1 H), 7.70 (d, J = 8.5 Hz, 1 H), 7.62−7.60 (m, 1 H), 7.47 (d, J = 8.0 Hz, 1 H), 6.62 (dd, J = 3.4, 1.6 Hz, 1 H), 3.57 (s, 2 H), 2.40−2.34

dx.doi.org/10.1021/jm500007h | J. Med. Chem. 2014, 57, 2692−2703

(m, 11 H), 2.19 (s, 3 H). ^{13}C NMR (125 MHz, DMSO-d_6) δ 165.29, 165.11, 160.91, 149.69, 142.77, 138.24, 138.13, 136.72, 132.22, 131.86, 131.18, 130.37, 128.02, 127.74, 127.47, 125.96, 125.09, 123.48, 122.04, 118.71, 117.26, 117.21, 100.97, 57.37, 54.59 (2C), 52.49 (2C), 45.49, 18.02. HRMS (ESI) calcd for $C_{29}H_{29}F_3N_6O_2$ [M + H]$^+$, 551.2377; found, 551.2375. HPLC purity = 96.06%, Rt 6.60 min.

***N*-(2-Methyl-5-((4-((4-methylpiperazin-1-yl)methyl)-3-(trifluoromethyl)phenyl)carbamoyl) phenyl)-1*H*-pyrazolo[3,4-b]pyridine-5-carboxamide 6b.** Yield: 42%. ^{1}H NMR (400 MHz, DMSO-d_6) δ 13.98 (s, 1 H), 10.48 (s, 1 H), 10.25 (s, 1 H), 9.12 (d, J = 1.9 Hz, 1 H), 8.88 (d, J = 1.9 Hz, 1 H), 8.35 (s, 1 H), 8.20 (s, 1 H), 8.08−8.03 (m, 2 H), 7.84 (d, J = 7.9 Hz, 1 H), 7.70 (d, J = 8.5 Hz, 1 H), 7.48 (d, J = 8.1 Hz, 1 H), 3.56 (s, 2 H), 2.48−2.23 (m, 11 H), 2.15 (s, 3 H). ^{13}C NMR (125 MHz, DMSO-d_6) δ 165.09, 164.52, 152.57, 148.71, 138.26, 138.13, 136.46, 134.65, 132.32, 131.87, 131.20, 130.46, 130.37, 127.51, 127.27, 125.95, 125.41, 123.50, 123.23, 117.29, 117.24, 113.62, 57.36, 54.55(2C), 52.41(2C), 45.40, 18.03. HRMS (ESI) calcd for $C_{28}H_{28}F_3N_7O_2$ [M + H]$^+$, 552.2330; found, 552.2331. HPLC purity = 97.48%, Rt 5.97 min.

***N*-(2-Methyl-5-((4-((4-methylpiperazin-1-yl)methyl)-3-(trifluoromethyl)phenyl)carbamoyl) phenyl)-1*H*-indole-5-carboxamide 6c.** Yield: 57%, ^{1}H NMR (400 MHz, DMSO-d_6) δ 13.36 (s, 1 H), 10.47 (s, 1 H), 10.07 (s, 1 H), 8.53 (s, 1 H), 8.28 (s, 1 H), 8.21 (d, J = 1.6 Hz, 1 H), 8.07 (dd, J = 8.4 Hz, 1.6 Hz, 1 H), 8.03 (d, J = 1.2 Hz, 1 H), 8.00 (dd, J = 8.8 Hz, 1.2 Hz, 1 H), 7.83 (dd, J = 8.0 Hz, 1.6 Hz, 1 H), 7.70 (d, J = 8.4 Hz, 1 H), 7.66 (d, J = 8.8 Hz, 1 H), 7.46 (d, J = 8.0 Hz, 1 H), 3.57 (s, 2 H), 2.50−2.34 (m, 11 H), 2.20 (s, 3 H). ^{13}C NMR (125 MHz, DMSO) δ 165.77, 165.13, 160.92, 141.06, 138.26, 138.16, 136.88, 134.92, 132.22, 131.84, 131.19, 130.35, 127.48, 126.66, 125.98, 125.48, 125.05, 123.48, 122.37, 121.24, 117.27, 109.95, 57.36, 54.56(2C), 52.43(2C), 45.42, 18.02. HRMS (ESI) calcd for $C_{30}H_{30}F_3N_5O_2$ [M + H]$^+$, 550.2425; found, 550.2425. HPLC purity = 98.24%, Rt 6.12 min.

***N*-(3-((4-((4-Methylpiperazin-1-yl)methyl)-3-(trifluoromethyl)phenyl)carbamoyl)phenyl)-1*H*-pyrrolo[2,3-b]-pyridine-5-carboxamide 6d.** Yield: 85%. ^{1}H NMR (400 MHz, DMSO-d_6) δ 12.02 (s, 1 H), 10.58 (s, 1 H), 10.52 (s, 1 H), 8.87 (d, J = 1.2 Hz, 1 H), 8.62 (s, 1 H), 8.39 (s, 1 H), 8.22 (s, 1 H), 8.08−8.04 (m, 2 H), 7.72 (s, 1 H), 7.70 (s, 1 H), 7.61 (t, J = 2.8 Hz, 1 H), 7.54 (t, J = 8.0 Hz, 1 H), 6.63 (d, J = 1.6 Hz, 1 H), 3.57 (s, 2 H), 2.39 (s, 8 H), 2.17 (s, 3 H). ^{13}C NMR (125 MHz, DMSO) δ 166.28, 165.92, 150.13, 143.28, 140.01, 138.66, 135.56, 132.46, 131.65, 129.11, 128.52, 128.23, 127.88(q, J = 30 Hz), 124.77(q, J = 274 Hz), 123.94, 120.28, 119.12, 117.64, 101.47, 57.87, 55.13(2C), 53.09(2C), 46.10; HRMS (ESI) calcd for $C_{28}H_{27}F_3N_6O_2$ [M + H]$^+$, 537.2221; found, 537.2220. HPLC purity = 99.14%, Rt 6.66 min.

***N*-(2-Ethyl-5-((4-((4-methylpiperazin-1-yl)methyl)-3-(trifluoromethyl)phenyl)carbamoyl)phenyl)-1*H*-pyrrolo[2,3-b]-pyridine-5-carboxamide 6e.** Yield: 42%. ^{1}H NMR (400 MHz, DMSO-d_6) δ 12.00 (s, 1 H), 10.49 (s, 1 H), 10.10 (s, 1 H), 8.88 (s, 1 H), 8.60 (s, 1 H), 8.21 (s, 1 H), 8.07 (d, J = 8.4 Hz, 1 H), 7.99 (s, 1 H), 7.89 (d, J = 7.6 Hz, 1 H), 7.70 (d, J = 8.4 Hz, 1 H), 7.61 (s, 1 H), 7.49 (d, J = 8.0 Hz, 1 H), 6.63 (s, 1 H), 3.56 (s, 2 H), 2.74 (dd, J = 14.4 Hz, 7.2 Hz, 2 H), 2.50−2.38 (m, 8 H), 2.16 (s, 3 H), 1.19 (t, J = 7.2 Hz, 3 H). ^{13}C NMR (125 MHz, DMSO) δ 166.32, 165.66, 150.04, 144.66, 143.12, 138.57, 136.41, 132.63, 132.39, 131.70, 129.17, 128.50, 128.23, 127.97, 127.74, 127.35, 126.20, 124.00, 123.63, 119.24, 117.72, 101.54, 57.77, 54.93(2C), 52.80(2C), 45.82, 24.47, 14.26; HRMS (ESI) calcd for $C_{30}H_{31}F_3N_6O_2$ [M + H]$^+$, 565.2534; found, 565.2533. HPLC purity = 95.37%, Rt 6.60 min.

***N*-(2-Isopropyl-5-((4-((4-methylpiperazin-1-yl)methyl)-3-(trifluoromethyl)phenyl)carbamoyl) phenyl)-1*H*-pyrrolo[2,3-b]pyridine-5-carboxamide 6f.** Yield: 28%. ^{1}H NMR (400 MHz, DMSO-d_6) δ 12.00 (s, 1 H), 10.48 (s, 1 H), 10.13 (s, 1 H), 8.89 (d, J = 2.0 Hz, 1 H), 8.62 (d, J = 1.6 Hz, 1 H), 8.21 (d, J = 1.6 Hz, 1 H), 8.07 (d, J = 8.4 Hz, 1 H), 7.94−7.92 (m, 2 H), 7.70 (d, J = 8.4 Hz, 1 H), 7.61 (t, J = 2.8 Hz, 1 H), 7.56 (d, J = 8.8 Hz, 1 H), 6.63 (dd, J = 3.2 Hz, 1.6 Hz, 1 H), 3.56 (s, 2 H), 3.33−3.27 (m, 1 H), 2.50−2.38 (m, 8 H), 2.16 (s, 3 H), 2.21 (d, J = 6.8 Hz, 6 H). ^{13}C NMR (125 MHz, DMSO-d_6) δ 165.96, 165.04, 149.70, 149.11, 142.75, 138.23, 135.31, 132.05, 131.92, 131.18, 127.96, 127.74, 127.51, 127.24, 126.19, 125.91, 123.48, 121.97, 118.73, 117.25, 117.20, 100.98, 57.40, 54.65(2C), 52.60(2C), 45.60, 27.76, 22.89(2C). HRMS (ESI) calcd for $C_{31}H_{33}F_3N_6O_2$ [M + H]$^+$, 579.2690; found, 579.2689. HPLC purity = 97.27%, Rt 7.10 min.

Methyl 2-(methylamino)pyrimidine-5-carboxylate 12b. To a solution of **11b** (1.05g, 5.58 mmol) in 6 mL of DMF, $Pd(OAc)_2$ (62.0 mg, 0.28 mmol), Xantphos (194.3 mg, 0.34 mmol), triethylamine (1.4 mL, 10.0 mmol), and 1.0 mL og methanol were added. The reaction flask was evacuated and backfilled with CO twice. The mixture was heated to 100 °C and stirred overnight under a CO balloon. Then, the reaction mixture was cooled to room temperature and diluted with water and extracted with ethyl acetate (3 × 50 mL). The combined organic layer was dried over anhydrous sodium sulfate, concentrated under vacuum, and was used in the next step without further purification. Compounds **12c−i** were synthesized by a similar procedure.

Methyl 2-(methylamino)pyrimidine-5-carboxylate 13b. To a solution of **12b** (446.0 mg, 0.27 mmol) in 15 mL of mixture solvent (MeOH/THF/H_2O = 3:3:9), LiOH (224.2 mg, 5.34 mmol) was added, and the resulting mixture was stirred at room temperature for 3 h. The organic solvent was removed under vacuum, and the resulting residue was diluted with water and extracted with ethyl acetate (2 × 50 mL). Then, the aqueous solution was acidified with dilute hydrochloric acid (pH about.4), and the precipitate was filtered and washed with water and petroleum ether to give the pure product **13b** (297.4 mg; yield, 73%). ^{1}H NMR (400 MHz, DMSO-d_6) δ 8.74 (d, J = 2.0 Hz, 1 H), 8.65 (d, J = 2.4 Hz, 1 H), 7.90 (d, J = 4.8 Hz, 1 H), 2.86 (d, J = 4.8 Hz, 3 H). MS (ESI), m/z 154 [M + H]$^+$.

2-(Ethylamino)pyrimidine-5-carboxylic Acid 13c. ^{1}H NMR (500 MHz, DMSO-d_6) δ 12.68 (s, 1 H), 8.72 (s, 1 H), 8.66 (s, 1 H), 7,99 (t, J = 5 Hz, 1 H), 3.38−3.32 (m, 2 H), 1.12 (t, J = 7 Hz, 3 H). MS (ESI), m/z 168 [M + H]$^+$.

2-(Cyclopropylamino)pyrimidine-5-carboxylic Acid 13e. ^{1}H NMR (400 MHz, DMSO-d_6) δ 12.74 (s, 1 H), 8.77 (s, 1 H), 8.67 (s, 1 H) 8.16 (d, J = 3.6 Hz, 1 H), 2.83−2.78 (m, 1 H), 0.73−0.68 (m, 2 H), 0.54 −0.50(m, 2 H); MS (ESI), m/z 180 [M + H]$^+$.

2-(Cyclopentylamino)pyrimidine-5-carboxylic Acid 13f. ^{1}H NMR (500 MHz, DMSO-d_6) δ 12.67 (s, 1 H), 8.71 (s, 1 H), 8.65 (s, 1 H), 8.03 (d, J = 7.5 Hz, 1 H), 4.25−4.21 (m, 1 H), 1.91−1.86 (m, 2 H), 1.71−1.1.65 (m, 2 H), 1.57−1.50 (m, 4 H); MS (ESI), m/z 208 [M + H]$^+$.

Compounds **13a−i** and **16a−c**[45] were synthesized by the same procedure; yield, 44−89%.

1*H*-Pyrrolo[2,3-*b*]pyridine-5-carboxylic Acid 16a. ^{1}H NMR (400 MHz, DMSO-d_6) δ 12.01 (s, 1 H), 8.78 (d, J = 1.8 Hz, 1 H), 8.50 (d, J = 1.8 Hz, 1 H), 7.58 (dd, J = 3.2 Hz, 1.8 Hz, 1 H), 6.60 (dd, J = 3.2 Hz, 1.8 Hz, 1 H); MS (ESI), m/z 163 [M + H]$^+$.

1*H*-Pyrazolo[3,4-*b*]pyridine-5-carboxylic Acid 16b. ^{1}H NMR (400 MHz, DMSO-d_6) δ 13.99 (s, 1H), 9.02 (d, J = 2.0 Hz, 1 H), 8.79 (d, J = 2.0 Hz, 1 H), 8.30 (s, 1 H); MS (ESI), m/z 164 [M + H]$^+$.

Cell Culture. The human colorectal adenocarcinoma cell lines HT-29, HCT-116, Colo205, LOVO, and WiDr and malignant melanoma cell lines A375 and SK-MEL-28 were purchased from ATCC. HT-29 and HCT116 were maintained in McCoy's 5a with 10% FBS, Colo205, LOVO, and A375 were maintained in RPMI-1640, F12K, and DMEM with 10% FBS, respectively, while WiDr and SK-MEL-28 were grown in Eagle's minimum essential medium with 10% FBS. The drug **1** resistant cell line SK-MEL-28-PR30 was selected in our laboratory by exposing the parental SK-MEL-28 cells to increasing concentrations of drug **1** for 2 months (Supporting Information).

***In Vitro* Enzymatic Activity Assay.** EGFR, B-Raf^{V600E} (as B-Raf^{V599E} in supplier's catalogue), and the Z′-Lyte Kinase Assay Kit were purchased from Invitrogen. The experiments were performed according to the instructions of the manufacturer. The concentrations of different kinases were determined by optimization experiments, and the respective concentrations were EGFR (PV3872, Invitrogen), 0.43 μg/μL; and BRAF^{V600E} (PV4173, Invitrogen), 0.22 μg/μL. First, the compounds were diluted 3-fold from 5.1 × 10^{-9} M to 1 × 10^{-4} M in DMSO, and a 4× compound solution was prepared (4 μL of compound dissolved in 96 μL of water). Second, a 40 μM ATP

dx.doi.org/10.1021/jm500007h | J. Med. Chem. 2014, 57, 2692−2703

solution in 1.33× kinase buffer was prepared. Third, a kinase/peptide mixture containing 2× kinase and 4 μM Tyr 4 peptide (Invitrogen, PV3193) was prepared right before use.

For both EGFR and B-Raf assays, 10 μL of kinase reactions were made at first (including 2.5 μL of compound solution, 5 μL of kinase/peptide mixture, and 2.5 μL of ATP solution). The plate was mixed thoroughly and incubated for 1 h at room temperature. Then 5 μL of development solution was added to each well, and the plate was incubated for 1 h at room temperature; the nonphospho-peptides were cleaved at this time. In the end, 5 μL of stop reagent was loaded to stop the reaction. For the control setting, 5 μL of phospho-peptide solution instead of the kinase/peptide mixture was used as 100% of the phosphorylation control. 2.5 μL of 1.33 × kinase buffer instead of ATP solution was used as 100% inhibition control, and 2.5 μL of 4% DMSO instead of compound solution was used as the 0% inhibitor control. The plate was measured on an EnVision Multilabel Reader (Perkin-Elmer). Curve fitting and data presentations were performed using Graph Pad Prism, version 5.0. Every experiment was repeated at least 2 times.

For the B-Raf^{V600E} assay, the kinase/peptide mixture was prepared by diluting the Z′-LYTE Ser/Thr3 peptide (Invitrogen, PV3176) and three kinases (B-Raf, MAP2K1/MEK1 (Invitrogen, P3093), MAPK1/ERK2 (Invitrogen, PV3314)) in 1× kinase buffer, and a 0.2 μM Ser/Thr3 phospho-peptide solution was made by adding Z′-LYTE Ser/Thr3 Phospho-peptide to 1× kinase buffer. The final 10 μL reaction consists of 0.002 ng of B-Raf, 10 ng of inactive MAP2K1 (MEK1),100 ng of inactive MAPK1 (ERK2), and 2 μM Ser/Thr3 peptide in 1× kinase buffer.

Cell Proliferation and Growth Inhibition Assay. WiDr, A375, HT-29, SK-MEL-28, SK-MEL-28-PR30, HCT-116, and LOVO cells were cultured with the respective growth medium. Cells of log phase were used. One thousand to 3000 cells/well were seeded in 96-well plates with a 100 μL volume, and 6 parallels and 8 rows were designed. Compounds were dissolved to 10 μM with DMSO, and a 5-fold serial dilution of the compounds from 1×10^{-5} M to 0.64×10^{-9} M was performed. Two microliters of compound solution was added to 998 μL of growth medium, the mixture was vortexed sufficiently. One hundred microliters of the mixture was correspondingly added to the 96-well plate. Two microliters of DMSO instead of compound solution was used as the 0% inhibitor control. After coincubation for 68 h, 20 μL of MTT (5 mg/mL) was added. Four hours later, the supernatant was discarded completely, and 150 μL of DMSO was added. After shaking for 10 min, the plates were read in the Synergy HT (Bio Tek) at 570 nm. The data was calculated using Graph Pad Prism, version 4.0. The IC_{50} were fitted using a nonlinear regression model with a sigmoidal dose−response.

Western Blot. Cells (1×10^6) of WiDr, A375, HT-29, SK-MEL-28, and SK-MEL-28-PR30 were seeded into 6-cm dishes overnight. The medium was changed, and 3, 1, 0.3 μM **6a** was added the next day; medium with 1‰ DMSO was used as the control. Cells were exposed to treatment for different times. The dishes were washed twice using precold PBS, and 400 μL of RIPA was added then. After incubating plates on ice for 15 min, cells were scraped carefully and centrifuged for 10 min at 14,000*g* at 4 °C immediately, and lysates (the supernantant) were maintained at −70 °C. A BCA protein assay kit (23227, Thermo) was used to quantitate the cell lysates. Proper 5× loading buffer was loaded before use, and the samples were denatured by boiling. The same amount of quantitated sample was loaded, and proteins were transferred to the PVDF membrane (Milipore) then. After blocking for 1.0 h at room temperature, diluted primary antibody EGFR (CST, 2232), phospho-EGFR (Tyr1068) (CST, 2234), ERK (CST, 9102), phospho-ERK (t202/y204) (CST, 9101), and GAPDH (KC-5G5, KangChen) were added. A second antibody with horseradish peroxidase (HRP, sigma) conjugated was used then. Blots were developed by enhanced chemiluminescence (Thermo).

■ ASSOCIATED CONTENT

Supporting Information

^{1}H NMR and ^{13}C NMR for final compounds, biological data, and assay details. This material is available free of charge via the Internet at http://pubs.acs.org.

■ AUTHOR INFORMATION

Corresponding Author

*Tel: +86-20-32015276. Fax: +86-20-32015299. E-mail: ding_ke@gibh.ac.cn.

Author Contributions

‖H.C., Y.C., and L.Z. contributed equally to this work.

Notes

The authors declare no competing financial interest.

■ ACKNOWLEDGMENTS

We thank the National Natural Science Foundation (#21302186) and the Key Project on Innovative Drug of Guangdong Province (#2012A080201014) for their financial support.

■ ABBREVIATIONS USED

MAPK, mitogen-activated protein kinase signaling pathway; EGFR, epidermal growth factor receptor; Erk, extracellular signal-regulated kinase; PDGFR, Platelet-derived growth factor; Val (V), valine; Glu (E), glutamic acid; rt, room temperature; DIEA, *N*,*N*-diisopropylethylamine; PyBOP, benzotriazol-1-yl-oxytripyrrolidinophosphonium hexafluorophosphate; HATU, 1-[bis(dimethylamino)methylene]-1*H*-1,2,3-triazolo[4,5-b]-pyridinium 3-oxid hexafluorophosphate; MOA, mechanisms of action; FDA, Food and Drug Administration; IC_{50}, the half maximal (50%) inhibitory concentration (IC) of a substance; THF, tetrahydrofuran; DMSO, dimethyl sulfoxide; GAPDH, glyceraldehyde-3-phosphate dehydrogenase; DMF, *N*,*N*-dimethylformamide; MTT, 3-(4,5-dimethylthiazol-2-yl)-2,5-diphenyltetrazolium bromide

■ REFERENCES

(1) Peyssonnaux, C.; Eychene, A. The Raf/MEK/ERK pathway: new concepts of activation. *Biol. Cell* **2001**, *93*, 53−62.

(2) Dhillon, A. S.; Hagan, S.; Rath, O.; Kolch, W. MAP kinase signalling pathways in cancer. *Oncogene* **2007**, *26*, 3279−3290.

(3) Marais, R.; Marshall, C. J. Control of the ERK MAP kinase cascade by Ras and Raf. *Cancer Surv.* **1996**, *27*, 101−125.

(4) Garnett, M. J.; Marais, R. Guilty as charged: B-RAF is a human oncogene. *Cancer Cell* **2004**, *6*, 313−319.

(5) Davies, H.; Bignell, G. R.; Cox, C.; Stephens, P.; Edkins, S.; Clegg, S.; Teague, J.; Woffendin, H.; Garnett, M. J.; Bottomley, W.; Davis, N.; Dicks, N.; Ewing, R.; Floyd, Y.; Gray, K.; Hall, S.; Hawes, R.; Hughes, J.; Kosmidou, V.; Menzies, A.; Mould, C.; Parker, A.; Stevens, C.; Watt, S.; Hooper, S.; Wilson, R.; Jayatilake, H.; Gusterson, B. A.; Cooper, C.; Shipley, J.; Hargrave, D.; Pritchard-Jones, K.; Maitland, N.; Chenevix-Trench, G.; Riggins, G. J.; Bigner, D. D.; Palmieri, G.; Cossu, A.; Flanagan, A.; Nicholson, A.; Ho, J. W. C.; Leung, S. Y.; Yuen, S. T.; Weber, B. L.; Siegler, H. F.; Darrow, T. L.; Paterson, H.; Marais, R.; Marshall, C. J.; Wooster, R.; Stratton, M. R.; Futreal, P. A. Mutations of the BRAF gene in human cancer. *Nature* **2002**, *417*, 949−954.

(6) Yuen, S. T.; Davies, H.; Chan, T. L.; Ho, J. W.; Bignell, G. R.; Cox, C.; Stephens, P.; Edkins, S.; Tsui, W. W.; Chan, A. S.; Futreal, P. A.; Stratton, M. R.; Wooster, R.; Leung, S. Y. Similarity of the phenotypic patterns associated with BRAF and KRAS mutations in colorectal neoplasia. *Cancer Res.* **2002**, *62*, 6451−6455.

(7) Kimura, E. T.; Nikiforova, M. N.; Zhu, Z. W.; Knauf, J. A.; Nikiforov, Y. E.; Fagin, J. A. High prevalence of BRAF mutations in thyroid cancer: genetic evidence for constitutive activation of the RET/PTC-RAS-BRAF signaling pathway in papillary thyroid carcinoma. *Cancer Res.* **2003**, *63*, 1454−1457.
(8) Wellbrock, C.; Hurlstone, A. BRAF as therapeutic target in melanoma. *Biochem. Pharmacol.* **2010**, *80*, 561−567.
(9) Tuveson, D. A.; Weber, B. L.; Herlyn, M. BRAF as a potential therapeutic target in melanoma and other malignancies. *Cancer Cell* **2003**, *4*, 95−98.
(10) Tsai, J.; Lee, J. T.; Wang, W.; Zhang, J.; Cho, H.; Mamo, S.; Bremer, R.; Gillette, S.; Kong, J.; Haass, N. K.; Sproesser, K.; Li, L.; Smalley, K. S. M.; Fong, D.; Zhu, Y. L.; Marimuthu, A.; Nguyen, H.; Lam, B.; Liu, J.; Cheung, I.; Rice, J.; Suzuki, Y.; Luu, C.; Settachatgul, C.; Shellooe, R.; Cantwell, J.; Kim, S. H.; Schlessinger, J.; Zhang, K. Y. J.; West, B. L.; Powell, B.; Habets, G.; Zhang, C.; Ibrahim, P. N.; Hirth, P.; Artis, D. R.; Herlyn, M.; Bollag, G. Discovery of a selective inhibitor of oncogenic B-Raf kinase with potent antimelanoma activity. *Proc. Natl. Acad. Sci. U.S.A.* **2008**, *105*, 3041−3046.
(11) Rheault, T. R.; Stellwagen, J. C.; Adjabeng, G. M.; Hornberger, K. R.; Petrov, K. G.; Waterson, A. G.; Dickerson, S. H.; Mook, R. A.; Laquerre, S. G.; King, A. J.; Rossanese, O. W.; Arnone, M. R.; Smitheman, K. N.; Kane-Carson, L. S.; Han, C.; Moorthy, G. S.; Moss, K. G.; Uehling, D. E. Discovery of dabrafenib: a selective inhibitor of Raf kinases with antitumor activity against B-Raf-driven tumors. *ACS Med. Chem. Lett.* **2013**, *4*, 358−362.
(12) Bollag, G.; Tsai, J.; Zhang, J. Z.; Zhang, C.; Ibrahim, P.; Nolop, K.; Hirth, P. Vemurafenib: the first drug approved for BRAF-mutant cancer. *Nat. Rev. Drug Discovery* **2012**, *11*, 873−886.
(13) Ballantyne, A. D.; Garnock-Jones, K. P. Dabrafenib: first global approval. *Drugs* **2013**, *73*, 1367−1376.
(14) Chapman, P. B.; Hauschild, A.; Robert, C.; Haanen, J. B.; Ascierto, P.; Larkin, J.; Dummer, R.; Garbe, C.; Testori, A.; Maio, M.; Hogg, D.; Lorigan, P.; Lebbe, C.; Jouary, T.; Schadendorf, D.; Ribas, A.; O'Day, S. J.; Sosman, J. A.; Kirkwood, J. M.; Eggermont, A. M.; Dreno, B.; Nolop, K.; Li, J.; Nelson, B.; Hou, J.; Lee, R. J.; Flaherty, K. T.; McArthur, G. A. Improved survival with vemurafenib in melanoma with BRAF V600E mutation. *N. Engl. J. Med.* **2011**, *364*, 2507−2516.
(15) Flaherty, K. T.; Puzanov, I.; Kim, K. B.; Ribas, A.; McArthur, G. A.; Sosman, J. A.; O'Dwyer, P. J.; Lee, R. J.; Grippo, J. F.; Nolop, K.; Chapman, P. B. Inhibition of mutated, activated BRAF in metastatic melanoma. *N. Engl. J. Med.* **2010**, *363*, 809−819.
(16) Sosman, J. A.; Kim, K. B.; Schuchter, L.; Gonzalez, R.; Pavlick, A. C.; Weber, J. S.; McArthur, G. A.; Hutson, T. E.; Moschos, S. J.; Flaherty, K. T.; Hersey, P.; Kefford, R.; Lawrence, D.; Puzanov, I.; Lewis, K. D.; Amaravadi, R. K.; Chmielowski, B.; Lawrence, H. J.; Shyr, Y.; Ye, F.; Li, J.; Nolop, K. B.; Lee, R. J.; Joe, A. K.; Ribas, A. Survival in BRAF V600-mutant advanced melanoma treated with vemurafenib. *N. Engl. J. Med.* **2012**, *366*, 707−714.
(17) Falchook, G. S.; Long, G. V.; Kurzrock, R.; Kim, K. B.; Arkenau, T. H.; Brown, M. P.; Hamid, O.; Infante, J. R.; Millward, M.; Pavlick, A. C.; O'Day, S. J.; Blackman, S. C.; Curtis, C. M.; Lebowitz, P.; Ma, B.; Ouellet, D.; Kefford, R. F. Dabrafenib in patients with melanoma, untreated brain metastases, and other solid tumours: a phase 1 dose-escalation trial. *Lancet* **2012**, *379*, 1893−1901.
(18) Hauschild, A.; Grob, J. J.; Demidov, L. V.; Jouary, T.; Gutzmer, R.; Millward, M.; Rutkowski, P.; Blank, C. U.; Miller, W. H., Jr.; Kaempgen, E.; Martin-Algarra, S.; Karaszewska, B.; Mauch, C.; Chiarion-Sileni, V.; Martin, A. M.; Swann, S.; Haney, P.; Mirakhur, B.; Guckert, M. E.; Goodman, V.; Chapman, P. B. Dabrafenib in BRAF-mutated metastatic melanoma: a multicentre, open-label, phase 3 randomised controlled trial. *Lancet* **2012**, *380*, 358−365.
(19) Johannessen, C. M.; Boehm, J. S.; Kim, S. Y.; Thomas, S. R.; Wardwell, L.; Johnson, L. A.; Emery, C. M.; Stransky, N.; Cogdill, A. P.; Barretina, J.; Caponigro, G.; Hieronymus, H.; Murray, R. R.; Salehi-Ashtiani, K.; Hill, D. E.; Vidal, M.; Zhao, J. J.; Yang, X. P.; Alkan, O.; Kim, S.; Harris, J. L.; Wilson, C. J.; Myer, V. E.; Finan, P. M.; Root, D. E.; Roberts, T. M.; Golub, T.; Flaherty, K. T.; Dummer, R.; Weber, B. L.; Sellers, W. R.; Schlegel, R.; Wargo, J. A.; Hahn, W. C.; Garraway, L. A. COT drives resistance to RAF inhibition through MAP kinase pathway reactivation. *Nature* **2010**, *468*, 968−972.
(20) Nazarian, R.; Shi, H. B.; Wang, Q.; Kong, X. J.; Koya, R. C.; Lee, H.; Chen, Z. G.; Lee, M. K.; Attar, N.; Sazegar, H.; Chodon, T.; Nelson, S. F.; McArthur, G.; Sosman, J. A.; Ribas, A.; Lo, R. S. Melanomas acquire resistance to B-RAF(V600E) inhibition by RTK or N-RAS upregulation. *Nature* **2010**, *468*, 973−977.
(21) Villanueva, J.; Vultur, A.; Lee, J. T.; Somasundaram, R.; Fukunaga-Kalabis, M.; Cipolla, A. K.; Wubbenhorst, B.; Xu, X. W.; Gimotty, P. A.; Kee, D.; Santiago-Walker, A. E.; Letrero, R.; D'Andrea, K.; Pushparajan, A.; Hayden, J. E.; Brown, K. D.; Laquerre, S.; McArthur, G. A.; Sosman, J. A.; Nathanson, K. L.; Herlyn, M. Acquired resistance to BRAF inhibitors mediated by a RAF kinase switch in melanoma can be overcome by cotargeting MEK and IGF-1R/PI3K. *Cancer Cell* **2010**, *18*, 683−695.
(22) Poulikakos, P. I.; Persaud, Y.; Janakiraman, M.; Kong, X. J.; Ng, C.; Moriceau, G.; Shi, H. B.; Atefi, M.; Titz, B.; Gabay, M. T.; Salton, M.; Dahlman, K. B.; Tadi, M.; Wargo, J. A.; Flaherty, K. T.; Kelley, M. C.; Misteli, T.; Chapman, P. B.; Sosman, J. A.; Graeber, T. G.; Ribas, A.; Lo, R. S.; Rosen, N.; Solit, D. B. RAF inhibitor resistance is mediated by dimerization of aberrantly spliced BRAF(V600E). *Nature* **2011**, *480*, 387−390.
(23) Shi, H. B.; Kong, X. J.; Ribas, A.; Lo, R. S. Combinatorial treatments that overcome PDGFR beta-driven resistance of melanoma cells to B-V600E-RAF inhibition. *Cancer Res.* **2011**, *71*, 5067−5074.
(24) Wagle, N.; Emery, C.; Berger, M. F.; Davis, M. J.; Sawyer, A.; Pochanard, P.; Kehoe, S. M.; Johannessen, C. M.; Macconaill, L. E.; Hahn, W. C.; Meyerson, M.; Garraway, L. A. Dissecting therapeutic resistance to RAF inhibition in melanoma by tumor genomic profiling. *J. Clin. Oncol.* **2011**, *29*, 3085−3096.
(25) Corcoran, R. B.; Ebi, H.; Turke, A. B.; Coffee, E. M.; Nishino, M.; Cogdill, A. P.; Brown, R. D.; Della Pelle, P.; Dias-Santagata, D.; Hung, K. E.; Flaherty, K. T.; Piris, A.; Wargo, J. A.; Settleman, J.; Mino-Kenudson, M.; Engelman, J. A. EGFR-mediated re-activation of MAPK signaling contributes to insensitivity of BRAF mutant colorectal cancers to RAF inhibition with vemurafenib. *Cancer Discovery* **2012**, *2*, 227−235.
(26) Prahallad, A.; Sun, C.; Huang, S. D.; Di Nicolantonio, F.; Salazar, R.; Zecchin, D.; Beijersbergen, R. L.; Bardelli, A.; Bernards, R. Unresponsiveness of colon cancer to BRAF(V600E) inhibition through feedback activation of EGFR. *Nature* **2012**, *483*, 100−103.
(27) Shi, H.; Moriceau, G.; Kong, X.; Koya, R. C.; Nazarian, R.; Pupo, G. M.; Bacchiocchi, A.; Dahlman, K. B.; Chmielowski, B.; Sosman, J. A.; Halaban, R.; Kefford, R. F.; Long, G. V.; Ribas, A.; Lo, R. S. Preexisting MEK1 exon 3 mutations in V600E/KBRAF melanomas do not confer resistance to BRAF inhibitors. *Cancer Discovery* **2012**, *2*, 414−424.
(28) Shi, H.; Moriceau, G.; Kong, X.; Lee, M. K.; Lee, H.; Koya, R. C.; Ng, C.; Chodon, T.; Scolyer, R. A.; Dahlman, K. B.; Sosman, J. A.; Kefford, R. F.; Long, G. V.; Nelson, S. F.; Ribas, A.; Lo, R. S. Melanoma whole-exome sequencing identifies (V600E)B-RAF amplification-mediated acquired B-RAF inhibitor resistance. *Nat. Commun.* **2012**, *3*, 724.
(29) Straussman, R.; Morikawa, T.; Shee, K.; Barzily-Rokni, M.; Qian, Z. R.; Du, J. Y.; Davis, A.; Mongare, M. M.; Gould, J.; Frederick, D. T.; Cooper, Z. A.; Chapman, P. B.; Solit, D. B.; Ribas, A.; Lo, R. S.; Flaherty, K. T.; Ogino, S.; Wargo, J. A.; Golub, T. R. Tumour micro-environment elicits innate resistance to RAF inhibitors through HGF secretion. *Nature* **2012**, *487*, 500−504.
(30) Antony, R.; Emery, C. M.; Sawyer, A. M.; Garraway, L. A. C-RAF mutations confer resistance to RAF inhibitors. *Cancer Res.* **2013**, *73*, 4840−4851.
(31) Lito, P.; Rosen, N.; Solit, D. B. Tumor adaptation and resistance to RAF inhibitors. *Nat. Med.* **2013**, *19*, 1401−1409.
(32) Kopetz, S.; Desai, J.; Chan, E.; Hecht, J. R.; O'Dwyer, P. J.; Lee, R. J.; Nolop, K. B.; Saltz, L. PLX4032 in metastatic colorectal cancer patients with mutant BRAF tumors. *J. Clin. Oncol.* **2010**, *28* (Suppl), a3534.

(33) Al-Marrawi, M. Y.; Saroya, B. S.; Brennan, M. C.; Yang, Z.; Dykes, T. M.; El-Deiry, W. S. Off-label use of cetuximab plus sorafenib and panitumumab plus regorafenib to personalize therapy for a patient with V600E BRAF-mutant metastatic colon cancer. *Cancer Biol. Ther.* **2013**, *14*, 703−710.
(34) Abel, E. V.; Basile, K. J.; Kugell, C. H., III; Witkiewicz, A. K.; Le, K.; Amaravadi, R. K.; Karakousis, G. C.; Xu, X.; Xu, W.; Schuchter, L. M.; Lee, J. B.; Ertel, A.; Fortina, P.; Aplin, A. E. Melanoma adapts to RAF/MEK inhibitors through FOXD3-mediated upregulation of ERBB3. *J. Clin. Invest.* **2013**, *123*, 2155−2168.
(35) DeVita, V. T.; Schein, P. S. The Use of drugs in combination for the treatment of cancer. *N. Engl. J. Med.* **1973**, *288*, 998−1006.
(36) Pegram, M. D.; Konecny, G. E.; O'Callaghan, C.; Beryt, M.; Pietras, R.; Slamon, D. J. Rational combinations of trastuzumab with chemotherapeutic drugs used in the treatment of breast cancer. *J. Natl. Cancer Inst.* **2004**, *96*, 739−749.
(37) Ribas, A.; Hodi, F. S.; Callahan, M.; Konto, C.; Wolchok, J. Hepatotoxicity with combination of vemurafenib and ipilimumab. *N. Engl. J. Med.* **2013**, *368*, 1365−1366.
(38) Rowbottom, M. W.; Faraoni, R.; Chao, Q.; Campbell, B. T.; Lai, A. G.; Setti, E.; Ezawa, M.; Sprankle, K. G.; Abraham, S.; Tran, L.; Struss, B.; Gibney, M.; Armstrong, R. C.; Gunawardane, R. N.; Nepomuceno, R. R.; Valenta, I.; Hua, H. L.; Gardner, M. F.; Cramer, M. D.; Gitnick, D.; Insko, D. E.; Apuy, J. L.; Jones-Bolin, S.; Ghose, A. K.; Herbertz, T.; Ator, M. A.; Dorsey, B. D.; Ruggeri, B.; Williams, M.; Bhagwat, S.; James, J.; Holladay, M. W. Identification of 1-(3-(6,7-dimethoxyquinazolin-4-yloxy)phenyl)-3-(5-(1,1,1-trifluoro-2-methylpropan-2-yl)isoxazol-3-yl)urea hydrochloride (CEP-32496), a highly potent and orally efficacious inhibitor of V-RAF murine sarcoma viral oncogene homologue B1 (BRAF) V600E. *J. Med. Chem.* **2012**, *55*, 1082−1105.
(39) Zhang, Q. W.; Diao, Y. Y.; Wang, F.; Fu, Y.; Tang, F.; You, Q. D.; Zhou, H. Y. Design and discovery of 4-anilinoquinazoline ureas as multikinase inhibitors targeting BRAF, VEGFR-2 and EGFR. *MedChemComm* **2013**, *4*, 979−986.
(40) Heffron, T. P.; Wei, B. Q.; Olivero, A.; Staben, S. T.; Tsui, V.; Do, S.; Dotson, J.; Folkes, A. J.; Goldsmith, P.; Goldsmith, R.; Gunzner, J.; Lesnick, J.; Lewis, C.; Mathieu, S.; Nonomiya, J.; Shuttleworth, S.; Sutherlin, D. P.; Wan, N. C.; Wang, S. M.; Wiesmann, C.; Zhu, B. Y. Rational design of phosphoinositide 3-kinase alpha inhibitors that exhibit selectivity over the phosphoinositide 3-kinase beta isoform. *J. Med. Chem.* **2011**, *54*, 7815−7833.
(41) Joseph, E. W.; Pratilas, C. A.; Poulikakos, P. I.; Tadi, M.; Wang, W. Q.; Taylor, B. S.; Halilovic, E.; Persaud, Y.; Xing, F.; Viale, A.; Tsai, J.; Chapman, P. B.; Bollag, G.; Solit, D. B.; Rosen, N. The RAF inhibitor PLX4032 inhibits ERK signaling and tumor cell proliferation in a V600E BRAF-selective manner. *Proc. Natl. Acad. Sci. U.S.A.* **2010**, *107*, 14903−14908.
(42) Wakeling, A. E.; Guy, S. P.; Woodburn, J. R.; Ashton, S. E.; Curry, B. J.; Barker, A. J.; Gibson, K. H. AZD1839 (Iressa): An orally active inhibitor of epidermal growth factor signaling with potential for cancer therapy. *Cancer Res.* **2002**, *62*, 5749−5754.
(43) Muhsin, M.; Graham, J.; Kirkpatrick, P. Gefitinib. *Nat. Rev. Drug Discovery* **2003**, *2*, 515−516.
(44) Jares-Erijman, E. A.; Jovin, T. M. FRET imaging. *Nat. Biotechnol.* **2003**, *21*, 1387−1395.
(45) Zheng, X. Z.; Bair, K. W.; Bauer, P.; Baumeister, T.; Bowman, K. K.; Buckmelter, A. J.; Caligiuri, M.; Clodfelter, K. H.; Feng, Y. Z.; Han, B. S.; Ho, Y. C.; Kley, N.; Li, H.; Liang, X. R.; Liederer, B. M.; Lin, J.; Ly, J.; O'Brien, T.; Oeh, J.; Oh, A.; Reynolds, D. J.; Sampath, D.; Sharma, G.; Skelton, N.; Smith, C. C.; Tremayne, J.; Wang, L. L.; Wang, W. R.; Wang, Z. G.; Wu, H. X.; Wu, J. S.; Xiao, Y.; Yang, G. X.; Yuen, P. W.; Zak, M.; Dragovich, P. S. Identification of amides derived from 1*H*-pyrazolo [3,4-*b*]pyridine-5-carboxylic acid as potent inhibitors of human nicotinamide phosphoribosyltransferase (NAMPT). *Bioorg. Med. Chem. Lett.* **2013**, *23*, 5488−5497.